Distinct and sequential tissue-specific activities of the LIM-class homeobox gene *Lim1* for tubular morphogenesis during kidney development

Akio Kobayashi[1,2], Kin-Ming Kwan[2], Thomas J. Carroll[3], Andrew P. McMahon[3], Cathy L. Mendelsohn[4] and Richard R. Behringer[1,2,*]

[1]Program in Developmental Biology, Baylor College of Medicine, Houston, TX 77030, USA
[2]Department of Molecular Genetics, University of Texas, M. D. Anderson Cancer Center, Houston, TX 77030, USA
[3]Department of Molecular and Cellular Biology, Harvard University, Cambridge, MA 02138, USA
[4]Department of Urology, Columbia University, College of Physicians and Surgeons, New York, NY 10032, USA
*Author for correspondence (e-mail: rrb@mdanderson.org)

Accepted 18 April 2005

Development 132, 2809-2823
Published by The Company of Biologists 2005
doi:10.1242/dev.01858

Summary

Kidney organogenesis requires the morphogenesis of epithelial tubules. Inductive interactions between the branching ureteric buds and the metanephric mesenchyme lead to mesenchyme-to-epithelium transitions and tubular morphogenesis to form nephrons, the functional units of the kidney. The LIM-class homeobox gene *Lim1* is expressed in the intermediate mesoderm, nephric duct, mesonephric tubules, ureteric bud, pretubular aggregates and their derivatives. *Lim1*-null mice lack kidneys because of a failure of nephric duct formation, precluding studies of the role of *Lim1* at later stages of kidney development. Here, we show that *Lim1* functions in distinct tissue compartments of the developing metanephros for both proper development of the ureteric buds and the patterning of renal vesicles for nephron formation. These observations suggest that *Lim1* has essential roles in multiple steps of epithelial tubular morphogenesis during kidney organogenesis. We also demonstrate that the nephric duct is essential for the elongation and maintenance of the adjacent Müllerian duct, the anlage of the female reproductive tract.

Key words: *Lhx1*, *Lim1*, Mesonephros, Metanephros, Müllerian duct

Introduction

Development of the kidney is one of the best-studied processes of vertebrate organogenesis (Grobstein, 1953; Grobstein, 1956; Kuure et al., 2000; Saxen, 1987; Vainio and Lin, 2002). This developmental process includes extensive tubular morphogenesis, including mesenchyme-to-epithelium transition, tubular elongation, branching and differentiation (Dressler, 2002; Hogan and Kolodziej, 2002; Lubarsky and Krasnow, 2003). During embryogenesis, the urogenital system derives from the intermediate mesoderm of the gastrula. Nephric ducts are paired epithelial tubes, formed in the intermediate mesoderm in an anteroposterior direction, that join the cloaca (Obara-Ishihara et al., 1999). The primary kidney, the pronephros, is formed at the anterior region of the nephric duct (Bouchard et al., 2002; Saxen, 1987). Subsequently, the secondary kidney, the mesonephros, is formed posterior to the pronephros (Sainio et al., 1997; Sainio and Raatikainen-Ahokas, 1999; Saxen, 1987). In amniotes (birds, reptiles, and mammals), the pronephros and mesonephros are transient embryonic kidneys that subsequently degenerate. The development of the amniote-specific definitive kidney, the metanephros, is initiated by induction of the ureteric bud at the posterior end of the nephric duct by signals from the adjacent metanephric mesenchyme that in mice occurs at approximately embryonic day 10.5 (E10.5). Subsequently, the ureteric bud elongates and branches to form the renal collecting duct system (Davies, 2001; Davies and Davey, 1999; Pohl et al., 2000; Shah et al., 2004). The metanephric mesenchyme, from which nephrons are derived, is reciprocally induced by the ureteric bud to form the condensed (induced) mesenchyme around the tip of the ureteric bud. Subsequently, a subset of cells in the condensed mesenchyme proliferates and forms the pretubular aggregate (Bard et al., 2001; Sariola, 2002; Stark et al., 1994). The renal vesicle is formed from the pretubular aggregate by a mesenchyme-to-epithelium transition and further differentiates into comma- and S-shaped bodies, and ultimately Bowman's capsule of the glomerulus and the tubules of the nephron (Saxen, 1987). How the nephron precursors are patterned to generate distinct cell types of the different physiological compartments of the nephron is not well understood.

To understand tissue-specific gene function in kidney organogenesis, in vitro tissue recombination assays have been used by culturing the ureteric bud and metanephric mesenchyme from wild-type and mutant animals (Grobstein, 1953; Grobstein, 1956; Miyamoto et al., 1997). However, this technique is limited if mutants die before metanephros

induction occurs or fail to form the ureteric bud or metanephric mesenchyme. Moreover, some cell types in the metanephros (e.g. endothelial cells and neurons) are not generated in the metanephros cultured in vitro (Vainio and Lin, 2002). Recently, conditional knockout strategies including the Cre-*loxP* recombination system in mice have been developed, which enables the study of tissue-specific gene function in vivo, avoiding embryonic lethality and/or early defects in precursor tissues (Kwan, 2002; Nagy, 2000).

The nephric duct also differentiates into the Wolffian duct, the primordium of the male reproductive tract that includes the epididymis, vas deferens and seminal vesicle. Subsequently, the Müllerian duct, the primordium of the oviduct, uterus and vagina of the female reproductive tract, is formed adjacent to the Wolffian duct in both male and female embryos before sexual dimorphic differentiation occurs (Kobayashi and Behringer, 2003). Thus, the formation of the genital ducts of the reproductive system is linked with the development of the excretory system.

The LIM-class homeodomain transcription factor, Lim1 (Lhx1 – Mouse Genome Informatics), is expressed in a dynamic pattern throughout urinary system development (Barnes et al., 1994; Fujii et al., 1994; Karavanov et al., 1998; Kobayashi et al., 2004; Kume et al., 2000; Tsang et al., 2000). In the mouse, *Lim1* is expressed in the intermediate mesoderm at E7.5 and the nephric duct and mesonephric tubules by E10.5. *Lim1* is also expressed in the metanephros. *Lim1* is expressed in the tip of the ureteric bud in the cortical region. In metanephric mesenchyme-derived tissues, *Lim1* expression is observed in the pretubular aggregate, the comma- and S-shaped bodies, and the podocyte of the immature glomerulus, and diminishes in the mature glomerulus (Karavanov et al., 1998; Sariola, 2002). Although almost all *Lim1*-null mutants die around E10.0 because of failure of chorioallantoic fusion for placenta formation, a few rare *Lim1*-null neonates are born and lack the metanephros (Shawlot and Behringer, 1995). This agenesis of the metanephros results from the failure of proper formation of the nephric duct (Tsang et al., 2000), which secondarily causes the lack of metanephros induction. Because there is both embryonic lethality and failure of proper formation of the nephric duct in *Lim1*-null mutants prior to the initiation of metanephros development, *Lim1* function in development of the mesonephros and metanephros remains unclear.

Here, we have examined *Lim1* function in mesonephros and metanephros development by avoiding the early defects of *Lim1*-null mutants, using BAC transgene rescue, tissue-specific knockout and chimera analysis. Our results demonstrate sequential, dosage-sensitive and distinct tissue-specific roles for *Lim1* in tubular morphogenesis during kidney organogenesis.

Materials and methods

Mice

Rarb2-Cre was generated using a 4.8 kb DNA fragment from the 5′ promoter region of the *Rarb2* gene (Mendelsohn et al., 1991) fused with *Cre-Mt1pA* (Sauer and Henderson, 1990). BAC and *Rarb2-Cre* transgenic mice were generated by pronuclear injection of C57BL/6 (B6)×SJL F2 zygotes (Nagy et al., 2003). The 7.6 kb *Kpn*I-*Not*I *Rarb2-Cre-Mt1pA* fragment was isolated and injected at 2 ng/μl. BAC DNA was linearized with PI-*Sce*I, and injected at 0.2 ng/μl.

Lim1$^{lz/+}$ (Kania et al., 2000) and *Lim1*$^{flox/flox}$ (Kwan and Behringer, 2002) mice were maintained on a B6×129/SvEv mixed genetic background, *Lim*$^{neo/+}$ (Shawlot and Behringer, 1995) on a B6 congenic background, *Hoxb7-Cre*$^{tg/+}$ (Yu et al., 2002) on a B6 inbred genetic background, and *R26R* (Soriano, 1999) and *Wnt4*$^{+/-}$ (Stark et al., 1994) on a B6 x 129/Sv mixed background.

PCR genotyping

The following primers were used for genotyping mice by PCR. For BAC-rescued *Lim1* mutant mice: mLim1-Fw8, GGCTACCTAAGCAACAACTACA; PGK-FX3, AGACTGCCTTGGGAAAAGCGC; BAC-Fw5, GTAAAACAAGCCACAGTTCTGAC; BAC-Rv6, TATTCAGCTACTGTTCCGTCAGC; Rap-A, AGGACTGGGTGGCTTCCAACTCCCAGACAC; Rap-B, AGCTTCTCATTGCTGCGCGCCAGGTTCAGG; lacZ-A, GCATCGAGCTGGGTAATAAGGGTTGGCAAT; and lacZ-B, GACACCAGACCAACTGGTAATGGTAGCGAC (Lim1neo, ~230 bp; BAC, 281 bp; Rap, 590 bp; lacZ, 822 bp). For *Hoxb7-Cre*$^{tg/+}$ mice: mHoxb7-Fw1, TGGGCCGGGGTCACGTGGTCAGA; Cre-Rv2, CGACGATGAAGCATGTTTAGCTG (~500 bp). For *Rarb2-Cre*$^{tg/+}$ mice: Cre-Fw6, GAAACAGGGGCAATGGTGCGCCTGCTG; mMt1-Rv1, AGGAAGACGCTGGGTTGGTCCGATACT (~1.1 kb). *Lim1*$^{lz/+}$, *Lim1*$^{neo/+}$, *Lim1*$^{flox/flox}$ and *Wnt4*$^{+/-}$ mice were genotyped as described previously (Kobayashi et al., 2004; Kwan and Behringer, 2002; Stark et al., 1994).

X-gal staining of embryos

X-gal staining was performed as described (Nagy et al., 2003). For histological analysis, paraffin embedded tissues were sectioned at 7 μm and counterstained with 0.33% eosin Y.

Whole-mount in situ hybridization

Whole-mount in situ hybridization was performed as described (Shawlot and Behringer, 1995).

Mouse chimeras

Lim1$^{+/+}$; *R26*$^{tg/+}$ ↔ wild-type and *Lim1*$^{-/-}$; *R26*$^{tg/+}$ ↔ wild-type chimeric mice were generated as previously described (Shawlot et al., 1999).

Results

Lim1 expression in nephric duct epithelium- and nephric mesenchyme-derived tissues

Lim1 is expressed in multiple tubule-forming tissues during kidney organogenesis and the genital ducts of the reproductive system. We found that *Lim1-lacZ* knock-in (*Lim1*$^{lz/+}$) mice (Kania et al., 2000) recapitulated the complex endogenous *Lim1* expression patterns during kidney development (see Fig. S1 in the supplementary material). Briefly, at E7.5 and E8.5, *Lim1-lacZ* expression was detected in the lateral mesoderm that comprises the intermediate mesoderm and lateral plate, and subsequently this expression was restricted to the nephric duct epithelium that forms within the intermediate mesoderm by E9.5. At E10.5, *Lim1-lacZ* expression was observed in the epithelial mesonephric vesicles. At this stage, *Lim1-lacZ* is weakly expressed in the epithelium of the nephric duct, but upregulated in the ureteric bud. In the metanephros, *Lim1-lacZ* is expressed weakly in the growing ureteric bud in the cortical region of the metanephros but strongly in the pretubular aggregate. *Lim1-lacZ* expression persists in the pretubular aggregate-derivatives, including the comma- and S-shaped bodies, and Bowman's capsule of the immature glomerulus, but is downregulated in the mature glomerulus. *Lim1-lacZ*

expression is also detected in the epithelium of the Wolffian (mesonephric) and Müllerian (paramesonephric) ducts in both sexes.

Hypomorphic phenotypes in BAC-rescued *Lim1* mutants

Although most *Lim1*-null mutants die during embryogenesis around E10, there are rare homozygous mutants that can survive to birth, which appears to be influenced by genetic background (Kobayashi et al., 2004). Two male and four female *Lim1*-null neonates were generated and all lacked the anterior head, metanephros and ureter (Fig. 1D,H). *Lim1*-null males had normal appearing testes but lacked the male reproductive tract, and female *Lim1*-null mutants had normal ovaries but lacked the female reproductive tract (Fig. 1H and data not shown) (Kobayashi et al., 2004).

To understand *Lim1* function in urogenital system development, we rescued the embryonic lethality of *Lim1*-null mutants using a mouse *Lim1*-containing bacterial artificial chromosome (BAC) transgene. We identified a ~208 kb C57BL/6J strain BAC clone (RP23-123A17) with the *Lim1* locus centrally located (Fig. 1A). Five *Lim1* BAC transgenic founders were generated and bred with *Lim1* heterozygous mice of two different null alleles, $Lim1^{neo/+}$ and $Lim1^{lz/+}$, to place the BAC transgenes on a *Lim1*-null background (Fig. 1B). BAC-rescued *Lim1* mutants ($Lim1^{lz/neo}$; $BAC^{tg/+}$) were readily recovered at birth using two independent BAC transgenic lines (lines 5 and 7) (Fig. 1C).

We found that all BAC-rescued *Lim1* mutants died within 1 day of birth for both transgenic lines, and displayed hypomorphic phenotypes in tissues requiring *Lim1* for their development, including the head, kidney and Müllerian duct

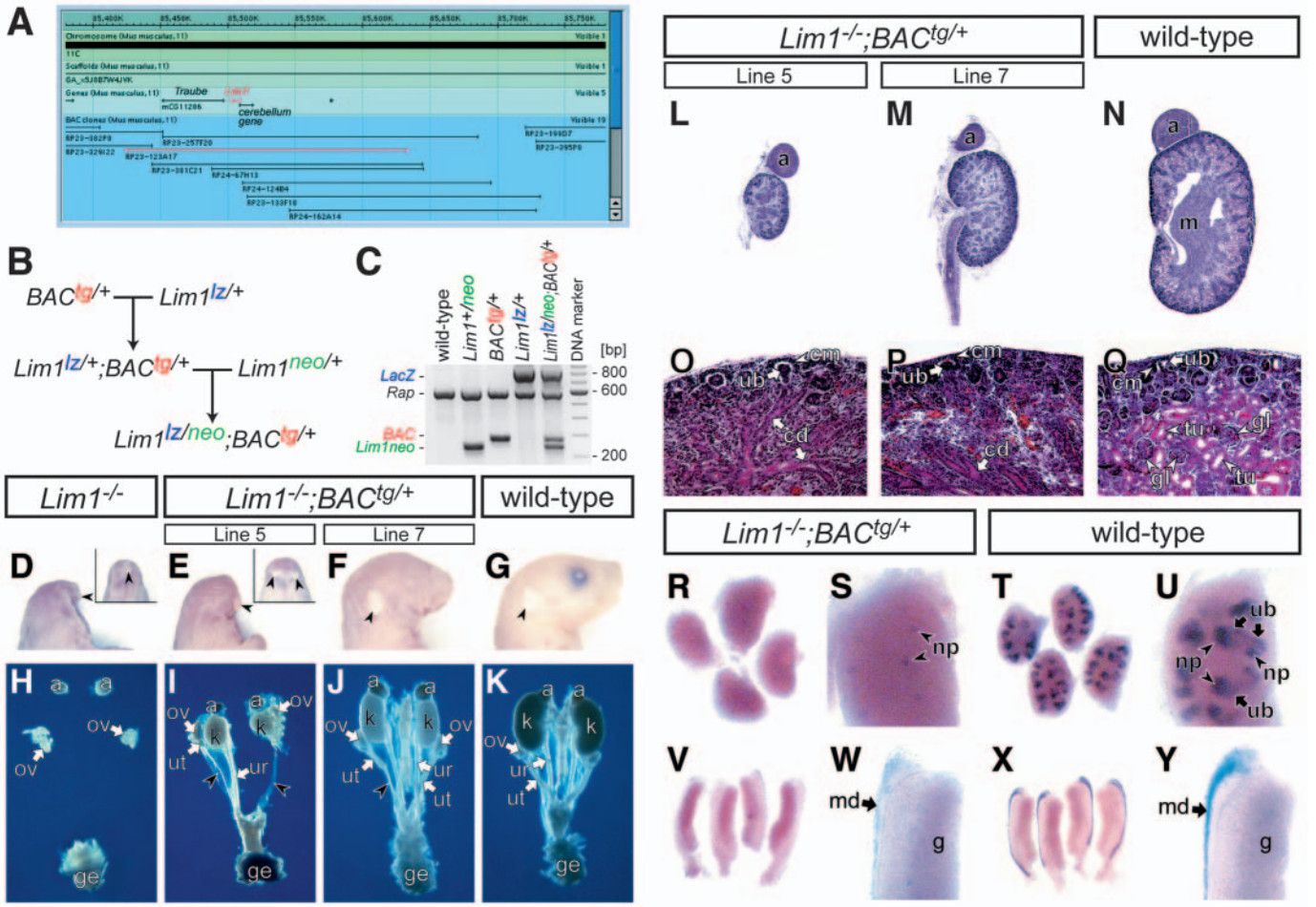

Fig. 1. Hypomorphic phenotypes in BAC transgene-rescued *Lim1* mutants. (A) Schematic diagram of mouse BAC clones around the *Lim1* locus. (Adapted, with permission, from Celera Discovery System.) (B) Breeding scheme to generate BAC transgene-rescued *Lim1* mutants. (C) PCR genotyping of neonates. Because two different null alleles of *Lim1* ($Lim1^{neo}$ and $Lim1^{lz}$) were used, BAC transgene-rescued *Lim1* mutants were easily identified by PCR genotyping. (D-Q) Phenotypes of *Lim1*-null (D,H), BAC transgene-rescued *Lim1* mutants for line 5 (E,I,L,O) and line 7 (F,J,M,P), and wild-type (G,K,N,Q) mice at birth. (D-G) Lateral view of the head region. Insets in D and E show frontal views. Arrowheads indicate ears. (H-K) Ventral view of urogenital system of female neonates. Arrowheads indicate connective tissues that lack the uterus, which is removed and not shown in H. (L-N) Hematoxylin and Eosin-stained metanephros. (O-Q) High magnification of the cortical region of the metanephros in L-N, respectively. (R-Y) Whole-mount in situ hybridization with a *Lim1* probe at E12.5 of the metanephros (R-U) and urogenital ridges (V-Y) from BAC transgene-rescued *Lim1* mutants (Line 7) (R,S,V,W) and wild-type (T,U,X,Y). (S,U,W,Y) High-magnification images in R, T, V and X. a, adrenal; cd, collecting duct; cm, condensed mesenchyme; g, gonad; ge, genitalia; gl, glomerulus; k, kidney; md, Müllerian duct; np, nephron progenitor; ov, ovary; tu, tubules of nephron; ub, ureteric bud; ur, ureter; ut, uterus.

derivatives (Fig. 1E,F,I,J). For line 7, some BAC-rescued *Lim1* mutants (21.7%, *n*=23) had craniofacial abnormalities, including a shortened snout, eye defects and loss of the lower jaw (Fig. 1F and data not shown). The female BAC-rescued mutants also frequently (46.2%, *n*=13) lacked the posterior part of the uterus (Fig. 1J). All of the BAC-rescued mutants for line 7 (*n*=23) had metanephroi that were smaller in comparison with wild-type controls (Fig. 1J,K). For line 5, the phenotypes of BAC-rescued *Lim1* mutants were more severe than line 7. All of the BAC-rescued *Lim1* mutants for line 5 (*n*=4) lacked most of the anterior head, which was smaller than those of rescued mutants for line 7 (Fig. 1E-G). These BAC-rescued *Lim1* mutants had two separate ears (Fig. 1E), whereas *Lim1*-null neonates usually have a single fused ear at the midline (Fig. 1D). All of the BAC-rescued *Lim1* mutants for line 5 lacked most of the uterus in females (*n*=3) (Fig. 1I) and had smaller metanephroi in both sexes (*n*=4) than those of BAC-rescued *Lim1* mutants for line 7 or wild type (Fig. 1I-K).

All of the BAC-rescued *Lim1* mutants for both transgenic lines 5 and 7 (*n*=27) had a shrunken bladder without urine (data not shown), suggesting that the smaller metanephroi were not functional. Histological analysis of the metanephroi of BAC-rescued *Lim1* mutants suggested retarded development of the ureteric bud and abnormalities of the medulla (Fig. 1L-N), although collecting ducts (the ducts of Bellini) were present (Fig. 1O-Q). The metanephros of BAC-rescued *Lim1* mutants also completely lacked nephrons, including glomeruli and associated tubules of the nephron as well as comma- and S-shaped bodies (Fig. 1O-Q).

Using line 7, we examined *Lim1* expression in BAC-rescued *Lim1* mutants. The level of BAC-derived *Lim1* expression was very low in all organs examined, including the metanephros, Müllerian duct and neural tube (Fig. 1R-Y, data not shown).

Nephric duct epithelium- and nephric mesenchyme-specific Cre transgenic mice

Lim1 is expressed in both ureteric bud- or metanephric mesenchyme-derived tissues and both ureteric bud- or metanephric mesenchyme-derived tissues have defects in BAC-rescued *Lim1* mutants. Because there are reciprocal interactions between these tissues, it is not clear if *Lim1* activity is required in the ureteric bud- or metanephric mesenchyme-derived tissues, or both. Therefore, we inactivated *Lim1* function individually in two distinct tissues of the metanephros using the Cre-*loxP* recombination system in vivo to bypass the nephric duct defect and early lethality of *Lim1*-null mutants.

For *Lim1* inactivation in nephric duct- and ureteric bud-derived tissues, we used *Hoxb7-Cre* transgenic mice (Yu et al., 2002). To inactivate *Lim1* in the nephric mesenchyme, including the metanephric mesenchyme, we generated a new Cre transgenic mouse line using a retinoic acid receptor β isoform 2 (*Rarb2*) gene promoter (Mendelsohn et al., 1991). To examine Cre recombinase activity in these transgenic mice, we crossed them with R26R Cre reporter mice (Soriano, 1999). Cre reporter expression was detected in the urogenital system from E9.5 in both *Hoxb7*- and *Rarb2-Cre* mice (Fig. 2A,B). For *Hoxb7-Cre*, reporter expression was detected in the entire nephric duct epithelium, but not in the nephric mesenchyme, at E9.5 (Fig. 2A,C). At the same stage, for *Rarb2-Cre*, reporter expression was restricted to the nephric mesenchyme in the anterior region of the mesonephros, but not in the nephric duct epithelium (Fig. 2B,D). Reporter expression for *Rarb2-Cre* was also detected in the anterior central nervous system (Fig. 2B; data not shown).

At E10.5, *Hoxb7-Cre* reporter expression remains restricted to the nephric duct epithelium, including the ureteric bud (Fig. 2E,G,I,K). At the same stage, *Rarb2-Cre* reporter expression extended posteriorly along the entire nephric duct mesenchyme, but not in the ureteric bud except for a few rare cells (Fig. 2F,H,J,L; data not shown). It has been proposed that cranial mesonephric tubules are derived from the nephric duct and caudal mesonephric tubules are derived from the nephric mesenchyme (Sainio et al., 1997). Consistent with this, *Hoxb7-Cre* and *Rarb2-Cre* reporter expression were also detected in the cranial and caudal mesonephros, respectively (Fig. 2G,H). *Rarb2-Cre* reporter expression was also observed in the limb mesenchyme and neuroretina of the eye (Fig. 2F; data not shown).

At E12.5 and E14.5, *Hoxb7-Cre* reporter expression remained in the nephric duct epithelium derivatives such as the epithelium of the Wolffian duct, ureter and ureteric bud (Fig. 2M,O,Q,S,U,W). At the same stages, *Rarb2-Cre* reporter expression remains restricted to the metanephric mesenchyme derivatives, including the condensed mesenchyme, cortical stroma, pretubular aggregate, comma- and S-shaped bodies, Bowman's capsule, proximal and distal tubules of the nephron and mesenchyme of the ureter and reproductive tracts (Fig. 2P,R,V,X). *Rarb2-Cre* reporter expression was also detected in the gubernaculum (Fig. 2N,T). No Cre reporter expression was detected in medullary (inner) stromal cells and glomerular capillary cells that are surrounded by Bowman's capsule, which include endothelial and mesangial cells, in either *Hoxb7-Cre* or *Rarb2-Cre* mice (Fig. 2U-X).

Distinct urogenital system phenotypes in nephric duct epithelium- and nephric mesenchyme-specific *Lim1* knockout mice

Using the *Hoxb7*- and *Rarb2-Cre* mice with a *Lim1* conditional null (*flox*) allele, we inactivated *Lim1* function in nephric duct epithelium- or nephric mesenchyme-derived tissues during kidney development, respectively. In *Hoxb7-Cre*$^{tg/+}$; *Lim1*$^{lz/flox}$ mutants, we found that *Lim1* expression in the ureteric bud was absent but *Lim1* expression in the pretubular aggregate and its derivative tissues was detected (Fig. 3B,E). In *Rarb2-Cre*$^{tg/+}$; *Lim1*$^{lz/flox}$ mutants, *Lim1* expression in the pretubular aggregate-derived tissues was not detected but *Lim1* expression in the ureteric bud was intact (Fig. 3C,F).

When *Lim1* was inactivated specifically in nephric duct-derived tissues using *Hoxb7-Cre*, the *Hoxb7-Cre*$^{tg/+}$; *Lim1*$^{lz/flox}$ mutants were viable and could survive to adulthood. However, when *Lim1* in metanephric mesenchyme-derived tissues was specifically inactivated by *Rarb2-Cre,* all of the *Rarb2-Cre*$^{tg/+}$; *Lim1*$^{lz/flox}$ mutants died within the first day of birth. All other mice with genotypes including *Lim1*$^{lz/flox}$, *Hoxb7-Cre*$^{tg/+}$, *Rarb2-Cre*$^{tg/+}$, *Hoxb7-Cre*$^{tg/+}$; *Lim1*$^{flox/+}$ and *Rarb2-Cre*$^{tg/+}$; *Lim1*$^{flox/+}$ were phenotypically identical to wild type.

At birth, the *Hoxb7-Cre*$^{tg/+}$; *Lim1*$^{lz/flox}$ mutant neonates had small metanephroi (Fig. 3H,N). Urine was observed in the bladder (data not shown), suggesting that the smaller metanephroi were functional. In some *Hoxb7-Cre*$^{tg/+}$; *Lim1*$^{lz/flox}$ mutants (40.0%, *n*=15), hydronephrosis and hydroureter were

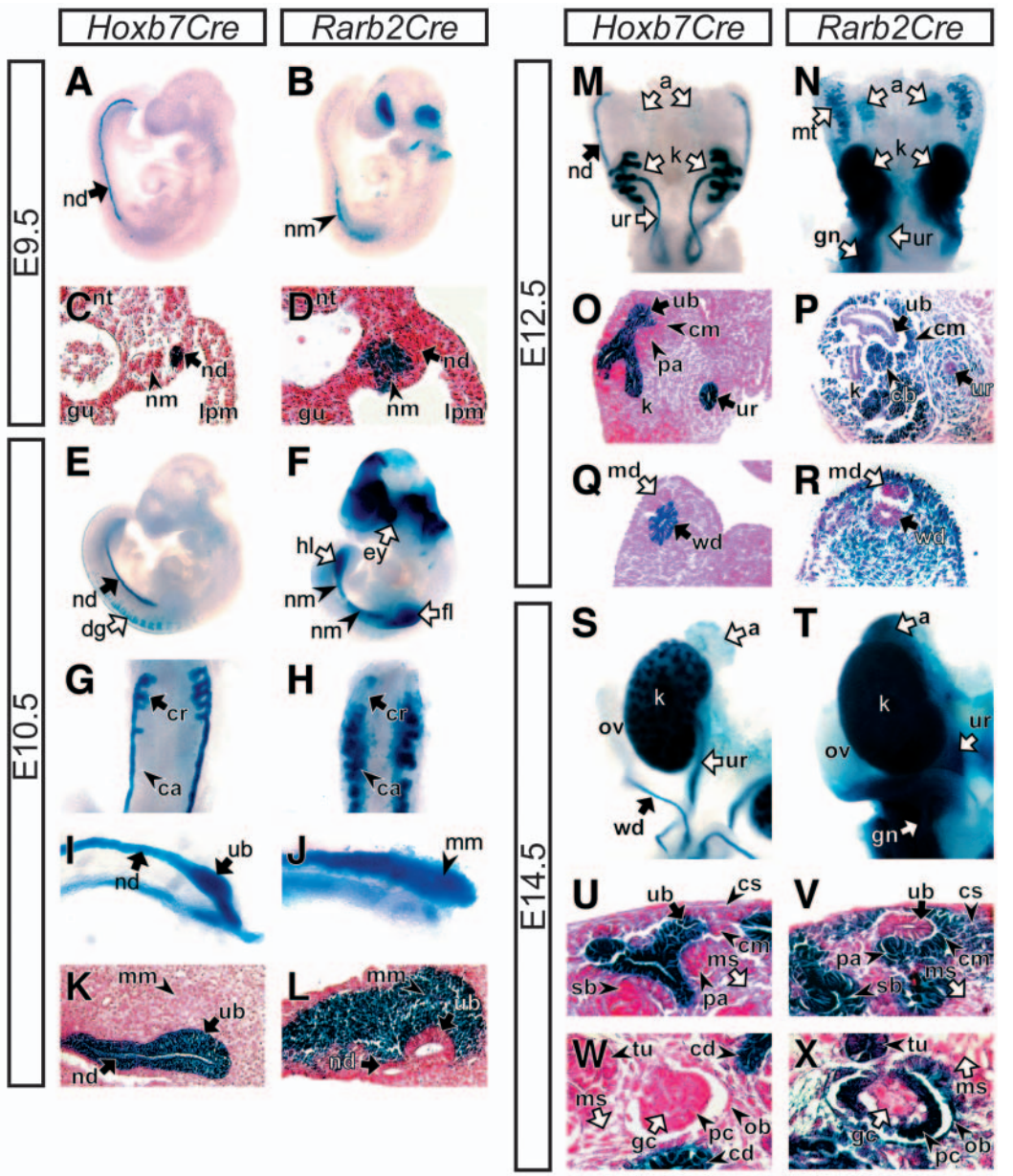

Fig. 2. Nephric duct epithelium- and metanephric mesenchyme-specific Cre reporter analysis. *lacZ* staining of *Hoxb7*$^{tg/+}$*; R26R*$^{+/-}$ (A,C,E,G,I,K,M,O,Q,S,U,W) and *Rarb2*$^{tg/+}$*; R26R*$^{+/-}$ (B,D,F,H,J,L,N,P,R,T,V,X) mice. (A,B) Whole-mount embryo at E9.5. (C,D) Cross-section of mesonephric region at E9.5. (E,F) Whole-mount embryo at E10.5. *Hoxb7-Cre* activity was also observed in the dorsal root ganglia and spinal cord (Yu et al. 2002). (G,H) Anterior region of the nephric duct at E10.5. (I,J) Posterior region of the nephric duct at E10.5. (K,L) Sagittal section around the posterior nephric duct region at E10.5. (M,N) Dorsal view of the urogenital system at E12.5. Mosaic *Hoxb7-Cre* and *Rarb2-Cre* reporter activity was observed in the adrenal gland. (O,P) Cross-section of the metanephros at E12.5. (Q,R) Cross-section of the posterior reproductive tracts. *Rarb2-Cre* reporter activity was mosaic in the mesenchyme of the posterior reproductive tracts. (S,T) Whole-mount urogenital system at E14.5. (U,V) Tip of ureteric bud in the cortical region of the metanephros at E14.5. (W,X) High magnification of the glomerulus at E14.5. a, adrenal; ca, caudal mesonephros; cb, comma-shaped body; cd, collecting duct; cm, condensed mesenchyme; cr, cranial mesonephros; cs, cortical (outer) stroma; dg, dorsal root ganglia; ey, eye; fl, forelimb; gc, glomerular capillaries; gl, glomerulus; gn, gubernaculum. gu, gut; hl, hindlimb; k, kidney (metanephros); lpm, lateral plate mesoderm; md, Müllerian duct; mm, metanephric mesenchyme; ms, medullary (inner) stroma; mt, mesonephric tubule; nd, nephric duct; nm, nephric mesenchyme; np, nephron progenitor; nt, neural tube; ob, outer layer of Bowman's capsule; ov, ovary; pa, pretubular aggregate; pc, podocyte; sb, S-shaped body; tu, tubules of nephron; ub, ureteric bud; ur, ureter; wd, Wolffian duct.

observed (Fig. 3N), suggesting urine production but abnormal development of the distal ureter, which results in obstruction of urinary excretion into the bladder (Batourina et al., 2002). Serial sections of these mice with hydronephrosis and hydroureter revealed that the distal ureter was closed in both sexes or ended abnormally into the uterus in some females (data not shown). These nephric duct-specific *Lim1* mutants also had abnormal reproductive tracts. In all *Hoxb7-Cre*$^{tg/+}$*; Lim1*$^{lz/flox}$ mutant males (n=8), most parts of the male reproductive tract such as the epididymis and vas deferens were absent, except for some residual tissue (Fig. 3K). In some *Hoxb7-Cre*$^{tg/+}$*; Lim1*$^{lz/flox}$ mutant females (57.1%, n=7), uteri were completely or partially absent with residual uterine tissue discontinuously present (Fig. 3Q and data not shown). The posterior uterus was more frequently absent compared with its anterior region (see Fig. S2 in the supplementary material; data not shown).

Rarb2-Cre$^{tg/+}$*; Lim1*$^{lz/flox}$ mutant neonates also had small metanephroi with normal ureters (n=10) (Fig. 3I,O). However, these small metanephroi were slightly bigger than those of *Hoxb7-Cre*$^{tg/+}$*; Lim1*$^{lz/flox}$ mutants (Fig. 3H,N). In addition, *Rarb2-Cre*$^{tg/+}$*; Lim1*$^{lz/flox}$ mutants had a shrunken bladder with no urine (data not shown). *Rarb2-Cre*$^{tg/+}$*; Lim1*$^{lz/flox}$ mice had normal reproductive tracts both in males and females (Fig. 3L,R).

Requirement of *Lim1* for formation and maintenance of the nephric duct

We found that the nephric duct was initially formed normally in *Hoxb7-Cre*$^{tg/+}$; *Lim1*$^{lz/flox}$ mice (Fig. 4C,F), which allowed induction of the metanephros by the ureteric bud and subsequent formation of the ureter (Fig. 3H,N). However, after formation of the nephric duct, *Lim1* expression in the nephric duct epithelium is inactivated by *Hoxb7-Cre* from E9.5 (Fig. 2A). The *Lim1*^{lz} reporter was used to follow *Lim1*-null cells in *Hoxb7-Cre*$^{tg/+}$; *Lim1*$^{lz/flox}$ mice. At E11.5, *Lim1-lacZ* expression in the nephric duct epithelium was discontinuous (Fig. 4H,J). Histological analysis of *Hoxb7-Cre*$^{tg/+}$; *Lim1*$^{lz/flox}$ mice revealed that the epithelial tissues of the nephric duct were not present where *lacZ* expression was absent (data not shown). This degeneration of the nephric duct epithelium results in the absence of most of the male reproductive tract such as the epididymis and vas deferens (Fig. 3K, Fig. 4R; see Fig. S2 in the supplementary material). The *Lim1-lacZ* reporter also revealed a loss of caudal mesonephric tubules, which are derived from the nephric mesenchyme (Fig. 2H), although the cranial mesonephros, which is derived from the nephric duct (Fig. 2G), was present (Fig. 4J).

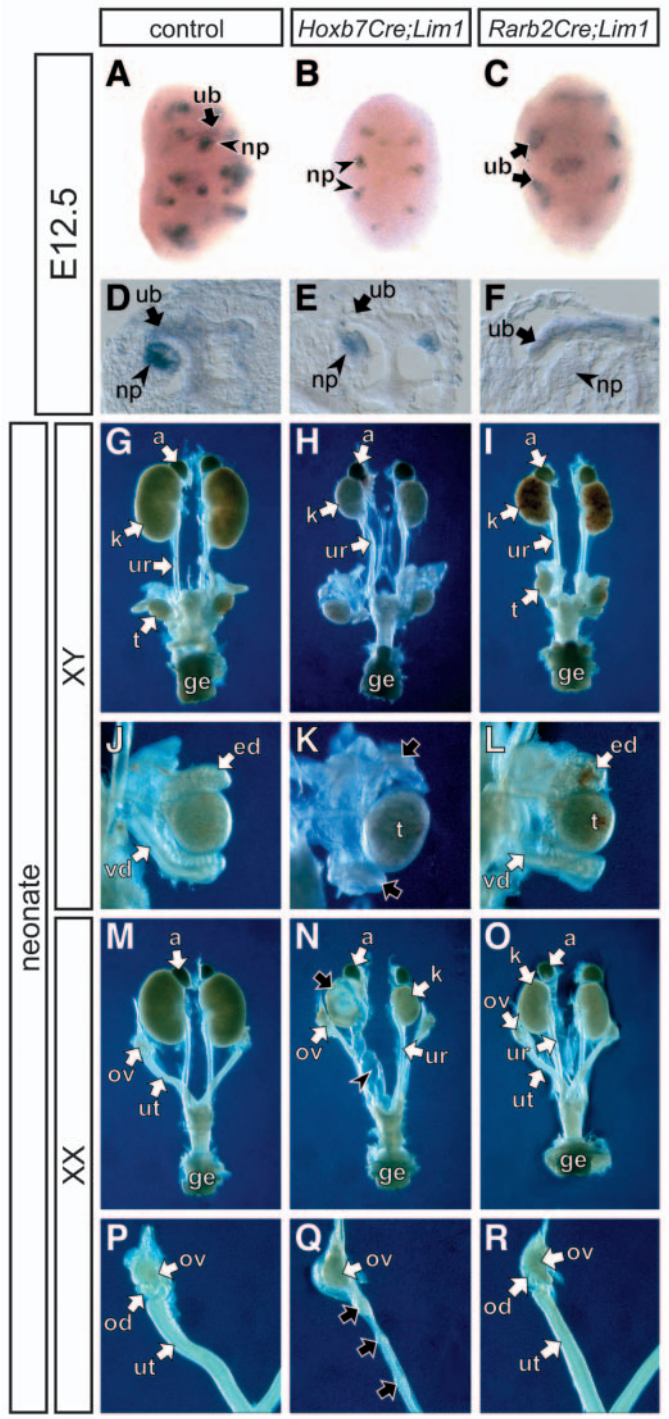

Müllerian duct defects caused by Wolffian duct loss

Lim1 expression is inactivated only in the nephric (Wolffian) duct epithelium, but not in the Müllerian duct of *Hoxb7-Cre*$^{tg/+}$; *Lim1*$^{lz/flox}$ mice (Fig. 2M,Q,S), which we confirmed by in situ hybridization (data not shown). However, we observed Müllerian aplasia in *Hoxb7-Cre*$^{tg/+}$; *Lim1*$^{lz/flox}$ mice (Fig. 3Q; see Fig. S2 in the supplementary material). In *Hoxb7-Cre*$^{tg/+}$; *Lim1*$^{lz/flox}$ mice, initiation of Müllerian duct formation was normal at E11.5 (Fig. 4H,J). However, posterior elongation of the Müllerian duct was impaired (Fig. 4L). Müllerian duct elongation was blocked where there was a discontinuity in the Wolffian duct (Fig. 4N). Interestingly the most anterior gaps of the Wolffian duct did not affect initial formation of the Müllerian duct (Fig. 4N, white arrowheads). After the Müllerian duct reaches the cloaca, the Wolffian duct further degenerates. We found that the Müllerian duct also starts to degenerate adjacent to where the Wolffian duct is lost (Fig. 4P).

Lim1 function in ureteric bud epithelium-derived tissues is essential for ureteric bud growth

The metanephros of *Hoxb7-Cre*$^{tg/+}$; *Lim1*$^{lz/flox}$ mice had morphologically normal medulla and glomeruli (Fig. 5B,F). However, the metanephroi of *Hoxb7-Cre*$^{tg/+}$; *Lim1*$^{lz/flox}$ mice was hypoplastic with reduced number of glomeruli (Fig. 3H,N; Fig. 5B,F; data not shown).

To understand *Lim1* function in the nephric duct epithelium derivatives, we examined *Lim1-lacZ* expression in the metanephros of *Hoxb7-Cre*$^{tg/+}$; *Lim1*$^{lz/flox}$ neonates. In neonates, *Lim1-lacZ* staining continues to show strong expression in the

Fig. 3. Urogenital abnormalities in tissue-specific knockout of *Lim1* in the nephric duct epithelium or nephric mesenchyme. (A-C) *Lim1* expression in the metanephros of tissue-specific *Lim1* mutants at E12.5. Nephric duct epithelium-specific *Lim1* knockout mice, *Hoxb7Cre*$^{tg/+}$; *Lim1*$^{lz/flox}$ (B), and metanephric mesenchyme-specific *Lim1* knockout mice, *Rarb2Cre*$^{tg/+}$; *Lim1*$^{lz/flox}$ (C). *Lim1*$^{lz/flox}$ (A) is shown for comparison. (D-F) Histological sections of A-C, respectively. (G-R) Phenotypes of the urogenital system of *Lim1*$^{lz/flox}$ (G,J,M,P), *Hoxb7Cre*$^{tg/+}$; *Lim1*$^{lz/flox}$ (H,K,N,Q) and *Rarb2Cre*$^{tg/+}$; *Lim1*$^{lz/flox}$ (I,L,O,R) neonates. Males (G-L) and females (M-R). (G-I) Ventral view of the urogenital system in male neonates. (J-L) Lateral view of the testicular region of male neonates. Black arrows in K indicate residual tissue of male reproductive tracts. (M-O) Ventral view of the urogenital system in female neonates. (N) Black arrow indicates hydronephrosis and the black arrowhead hydroureter. (P-R) High magnification of the anterior female reproductive tract region. Black arrows in Q indicate residual tissue of the uterus. a, adrenal; ed, epididymis; ge, genitalia; k, kidney (metanephros); np, nephron progenitor; od, oviduct; ov, ovary; t, testis; ub, ureteric bud; ur, ureter; ut, uterus; vd, vas deferens.

developing nephrons and weak expression in the ureteric bud (Fig. 5I,M). We found that the number of developing nephrons was greatly reduced at birth (Fig. 5J). Furthermore, the distribution of nephron progenitors is disorganized and there are scattered regions lacking nephron progenitors (Fig. 5J). In the metanephros of *Hoxb7-Cre$^{tg/+}$; Lim1$^{lz/flox}$* embryos, nephrons are found at every ureteric bud branching tip (Fig. 5R).

By tail somite (ts) stage 6, *Lim-lacZ* expression revealed that the nephric duct reaches the posterior region of the urogenital system adjacent to the metanephric mesenchyme in both control and *Hoxb7-Cre$^{tg/+}$; Lim1$^{lz/flox}$* embryos (Fig. 6A,B), which is consistent with the previous observation of normal formation of the nephric duct in *Hoxb7-Cre$^{tg/+}$; Lim1$^{lz/flox}$* embryos initially (Fig. 4F). However, induction of the ureteric bud is delayed in *Hoxb7-Cre$^{tg/+}$; Lim1$^{lz/flox}$* embryos (Fig. 6B), although *Lim1-lacZ* expression is upregulated for ureteric bud induction in the posterior part of the nephric duct (Fig. 6B).

Several molecules have been shown to be required for ureteric bud development (Carroll and McMahon, 2003; Lechner and Dressler, 1997; Pohl et al., 2000; Shah et al., 2004). *Ret* is required for formation, growth and branching of the ureteric bud (Schuchardt et al., 1994). It is weakly expressed in the nephric duct and its expression is upregulated in the ureteric bud tip (Fig. 6C). However, in *Hoxb7-Cre$^{tg/+}$; Lim1$^{lz/flox}$* embryos, the upregulation of *Ret* at the posterior region of the nephric duct was not as robust as their control littermates (Fig. 6D). Glial cell line-derived neurotrophic factor (GDNF) is a ligand for Ret expressed in the metanephric mesenchyme and is also required for ureteric bud formation, growth and branching (Moore et al., 1996; Pichel et al., 1996; Sanchez et al., 1996). We found that *Gdnf* is normally expressed in the metanephric mesenchyme of *Hoxb7-Cre$^{tg/+}$; Lim1$^{lz/flox}$* embryos at ts9 (Fig. 6G,H). Other molecular markers for the metanephric mesenchyme, such as *Eya1* and *Pax2*, were also normally detected in *Hoxb7-Cre$^{tg/+}$; Lim1$^{lz/flox}$* embryos at the same stage (Fig. 6I,J; data not shown). *Wnt11* is expressed in the tip of the ureteric bud (Kispert et al., 1996) and its

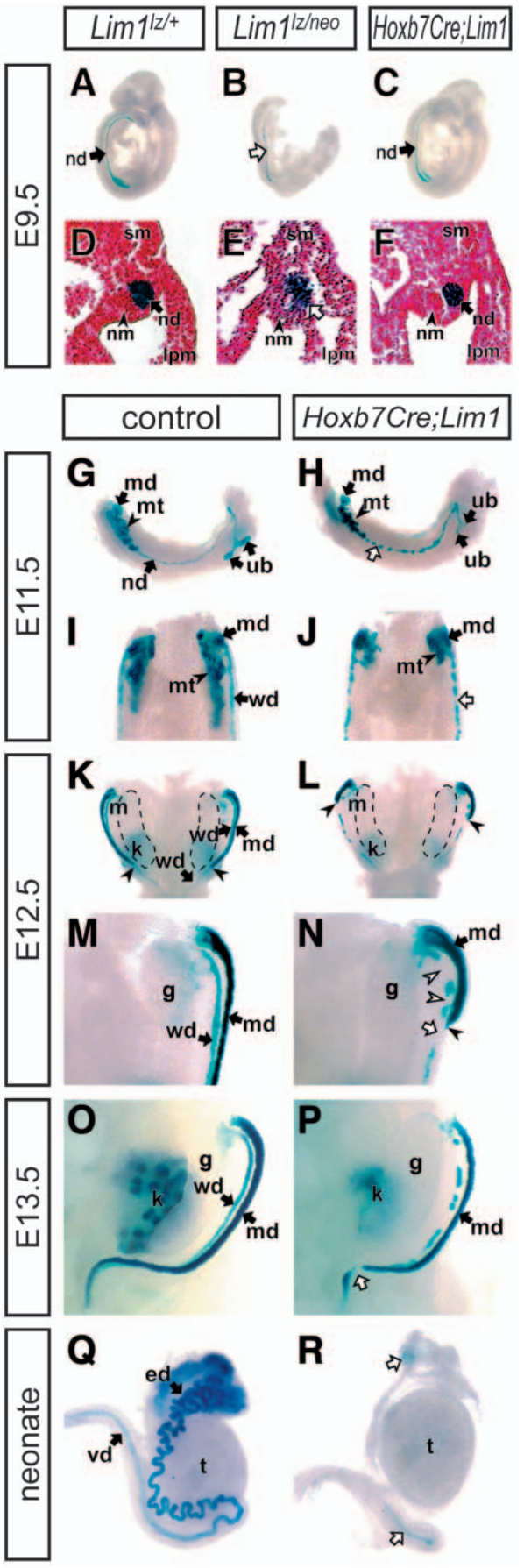

Fig. 4. Abnormal development of the reproductive tract in nephric duct epithelium-specific *Lim1* knockout mutants. (A-F) *Lim1-lacZ* expression in *Lim1$^{lz/+}$* (A,D), *Lim1$^{lz/neo}$* (B,E) and *Hoxb7Cre$^{tg/+}$; Lim1$^{lz/flox}$* (C,F) embryos at E9.5. (A-C) Lateral view of whole embryos. (D-F) Cross-sections of A-C, respectively. White arrows in B and E indicate disorganized *Lim1-lacZ*-positive cells in *Lim1*-null mutants, which form the epithelial tubule of the nephric duct in control (A,D) and *Hoxb7Cre$^{tg/+}$; Lim1$^{lz/flox}$* (C,F) mice. (G-R) *Lim1-lacZ* expression in developing urogenital organs of *Lim1$^{lz/flox}$* (G,I,K,M,O,Q) and *Hoxb7Cre$^{tg/+}$; Lim1$^{lz/flox}$* (H,J,L,N,P,R). (G-J) E11.5. (G,H) Lateral view of the urogenital system. (I,J) Ventral view of the mesonephros. White arrows in H and J indicate the degenerating nephric (Wolffian) duct. (K-N) E12.5. (K,L) Ventral view of the urogenital system. (M,N) Ventral view of the anterior mesonephros. Black arrowheads indicate the posterior end of the Müllerian duct; white arrow and arrowheads indicate gap in the Wolffian duct epithelium that inhibits or does not inhibit Müllerian duct elongation, respectively. (O,P) Ventral view of the left half of the urogenital system at E13.5. White arrow indicates gap in the Müllerian duct epithelium. (Q,R) Lateral view of the testis region at birth. White arrows indicate residual epithelium of the male reproductive tract. ed, epididymis; g, gonad; k, kidney (metanephros); lpm, lateral plate mesoderm; m, mesonephros; md, Müllerian duct; mt, mesonephric tubule; nd, nephric duct; nm, nephric mesenchyme; sm, somite; t, testis; ub, ureteric bud; vd, vas deferens; wd, Wolffian (nephric) duct.

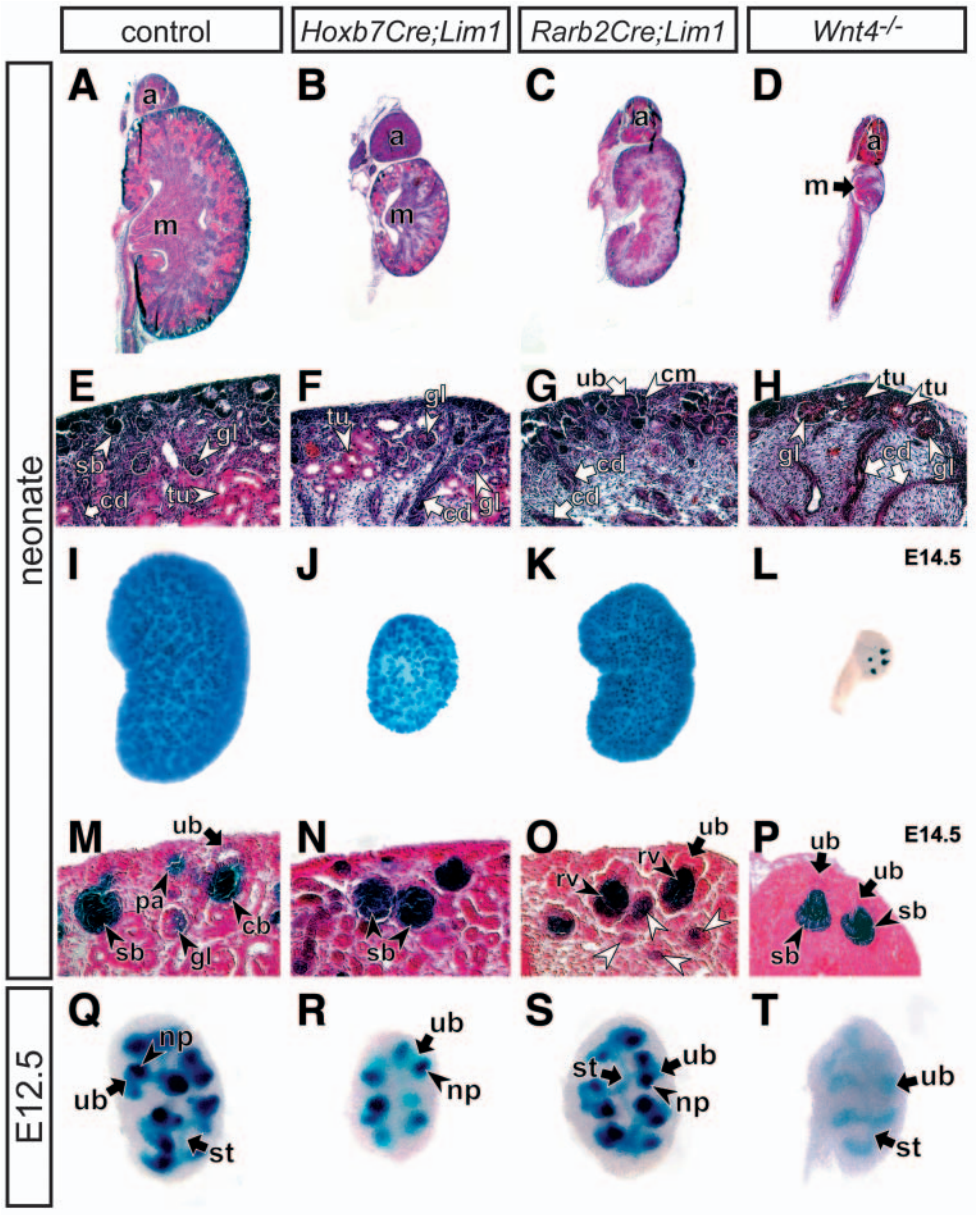

Fig. 5. Analysis of metanephros development in nephric duct epithelium- and metanephric mesenchyme-specific *Lim1* knockout mutants. Metanephros of nephric duct epithelium-specific *Lim1* knockout mice, *Hoxb7Cre*$^{tg/+}$*; Lim1*$^{lz/flox}$ (B,F,J,N,R) and metanephric mesenchyme-specific *Lim1* knockout mice, *Rarb2Cre*$^{tg/+}$*; Lim1*$^{lz/flox}$ (C,G,K,O,S). *Lim1*$^{lz/flox}$ (A,E,I,M,Q), *Wnt4*$^{-/-}$ (D,H) and *Wnt4*$^{-/-}$*; Lim1*$^{lz/+}$ (L,P,T) mice are shown for comparison. (A-P) Metanephros at birth, except for L and P (E14.5). (A-D) Hematoxylin and Eosin stained coronal sections. (E-H) High magnification of the cortical regions in A-D, respectively. (I-L) Ventral view of *Lim1-lacZ*-stained whole-mount metanephros. (M-P) Section of cortical region in I-L, respectively. White arrowheads in O indicate *Lim1-lacZ*-positive cells in degenerating renal vesicles. (Q-T) *Lim1-lacZ* stained whole-mount metanephros at E12.5. a, adrenal; cb, comma-shaped body; cd. collecting duct; cm, condensed mesenchyme; gl, glomerulus; m, medulla; np, nephron progenitor; pa, pretubular aggregate; rv, renal vesicle; sb, S-shaped body; st, stalk; tu, tubules of the nephron; ub, ureteric bud.

function is required for proper ureteric branching interacting with Ret (Majumdar et al., 2003). At ts9, *Wnt11* expression is detected in the swollen-shaped tip of the ureteric bud (Fig. 6E). Although the pattern of *Wnt11* expression appears thinner, its expression is correctly upregulated in the posterior nephric duct of *Hoxb7-Cre*$^{tg/+}$*; Lim1*$^{lz/flox}$ embryos (Fig. 6F).

At ts18, strong expression of *Ret* persists in wild-type ureteric bud tips (Fig. 6K). This *Ret* expression was not observed in the retarded ureteric bud of *Hoxb7-Cre*$^{tg/+}$*; Lim1*$^{lz/flox}$ mutants (Fig. 6L). At the same stage, *Wnt11* expression indicated that the ureteric bud tips persist in *Hoxb7-Cre*$^{tg/+}$*; Lim1*$^{lz/flox}$ embryos (Fig. 6O,P). However, *Lim1-lacZ* and *Wnt11* expression patterns revealed a shorter distance between two smaller ureteric bud tips (Fig. 6M-P), suggesting that ureteric bud growth is retarded in the metanephros of *Hoxb7-Cre*$^{tg/+}$*; Lim1*$^{lz/flox}$ embryos. The metanephric mesenchyme marker *Pax2* and the stroma marker *Bf2* (also known as *Foxd1*) (Hatini et al., 1996) are normally expressed in both wild-type and *Hoxb7-Cre*$^{tg/+}$*; Lim1*$^{lz/flox}$ mutants at this stage (data not shown).

Lim1 function in metanephric mesenchyme-derived tissue is essential for formation of the nephron, but not induction of nephron precursors

Histological analysis of the metanephroi of *Rarb2-Cre*$^{tg/+}$*; Lim1*$^{lz/flox}$ neonates revealed that the medulla was not correctly formed and there were no nephron tissues such as glomeruli and their associated tubules (Fig. 5C,G). However, *Lim1-lacZ* expression in the metanephros of *Rarb2-Cre*$^{tg/+}$*; Lim1*$^{lz/flox}$ embryos at E12.5 showed the presence of nephron progenitors (Fig. 5S).

Although the number of developing pretubular aggregates was slightly reduced in the smaller metanephroi of *Rarb2-Cre*$^{tg/+}$*; Lim1*$^{lz/flox}$ mutants, we found that the distribution pattern of the nephron progenitors was normal (Fig. 5K), in contrast to the abnormal pattern found in the metanephroi of *Hoxb7-Cre*$^{tg/+}$*; Lim1*$^{lz/flox}$ mice (Fig. 5J). Histological analysis revealed that nephron development is arrested at the stage of the renal vesicle, which are *Lim1-lacZ* positive (Fig. 5O). Apparently, these *Lim1-lacZ* positive tissues subsequently degenerate (Fig. 5O, white arrowheads).

It has previously been shown that *Wnt4*-null mutants also lack nephrons (Stark et al., 1994). Because *Lim1* and *Wnt4* are

co-expressed in the pretubular aggregate, it has been proposed that these genes may be involved in the same pathway for nephron development (Sariola, 2002). Therefore, we examined this possibility by comparing *Rarb2-Cre*$^{tg/+}$*; Lim1*$^{lz/flox}$ mutant mice with *Wnt4*-null mice. We found that the metanephroi of *Wnt4*-null mice were severely hypoplastic compared with those of *Rarb2-Cre*$^{tg/+}$*; Lim1*$^{lz/flox}$ mutant mice (Fig. 5C,D). Surprisingly, we also found that the small metanephroi of

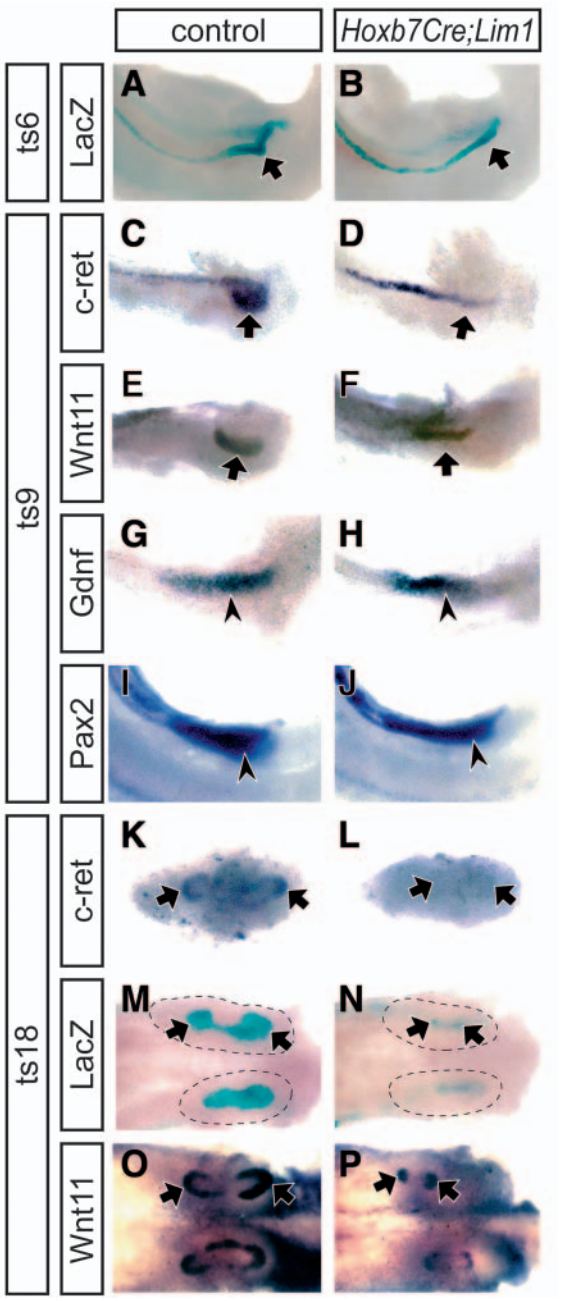

Fig. 6. Molecular expression analysis of nephric duct epithelium-specific *Lim1* knockout mutants. *Lim1*$^{lz/flox}$ (A,M), *Hoxb7Cre*$^{tg/+}$*; Lim1*$^{flox/+}$ (C,E,G,I,K,O) and *Hoxb7Cre*$^{tg/+}$*; Lim1*$^{lz/flox}$ (B,D,F,H,J,L,N,P) mice. (A-J) Lateral view of posterior nephric duct. (A,B) *Lim1-lacZ* expression at ts6. (C-J) Whole-mount in situ hybridization at ts9 with probes for *Ret* (C,D), *Wnt11* (E,F), *Gdnf* (G,H) and *Pax2* (I,J). Arrows indicate ureteric bud; arrowheads indicate metanephric mesenchyme. (K-P) Dorsal view of the metanephros at ts18 with *Ret* (K,L), *Lim1-lacZ* (M,N) and *Wnt11* (O,P) expression. Arrows indicate ureteric bud tips.

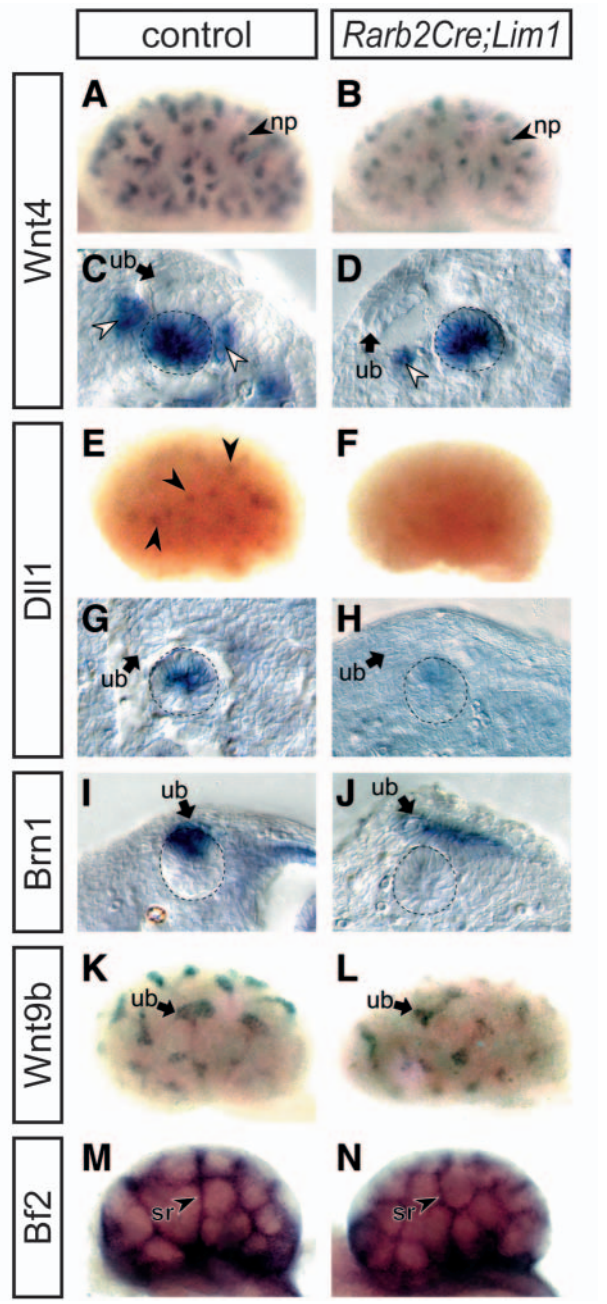

Fig. 7. Molecular expression analysis of metanephric mesenchyme-specific *Lim1* knockout mutants. Whole-mount in situ hybridization of the metanephros of *Rarb2Cre*$^{tg/+}$*; Lim1*$^{flox/+}$ (A,C,E,G,I,K,M) and *Rarb2Cre*$^{tg/+}$*; Lim1*$^{lz/flox}$ (B,D,F,H,J,L,N) embryos at E13.5 with *Wnt4* (A-D), *Dll1* (E-H), *Brn1* (I,J), *Wnt9b* (K,L) and *Bf2* (M,N) probes. (A,B,E,F,K-N) Ventral view of the metanephros. (C,D,G-J) Cryosection of the cortical region of the metanephros. Broken lines indicate renal vesicle; white arrowheads in C and D indicate *Wnt4*-expressing pretubular aggregate cells that do not form the renal vesicle; black arrowheads in E indicate *Dll1* upregulation in differentiated nephron progenitors. np, nephron progenitor; sr, stroma; ub, ureteric bud.

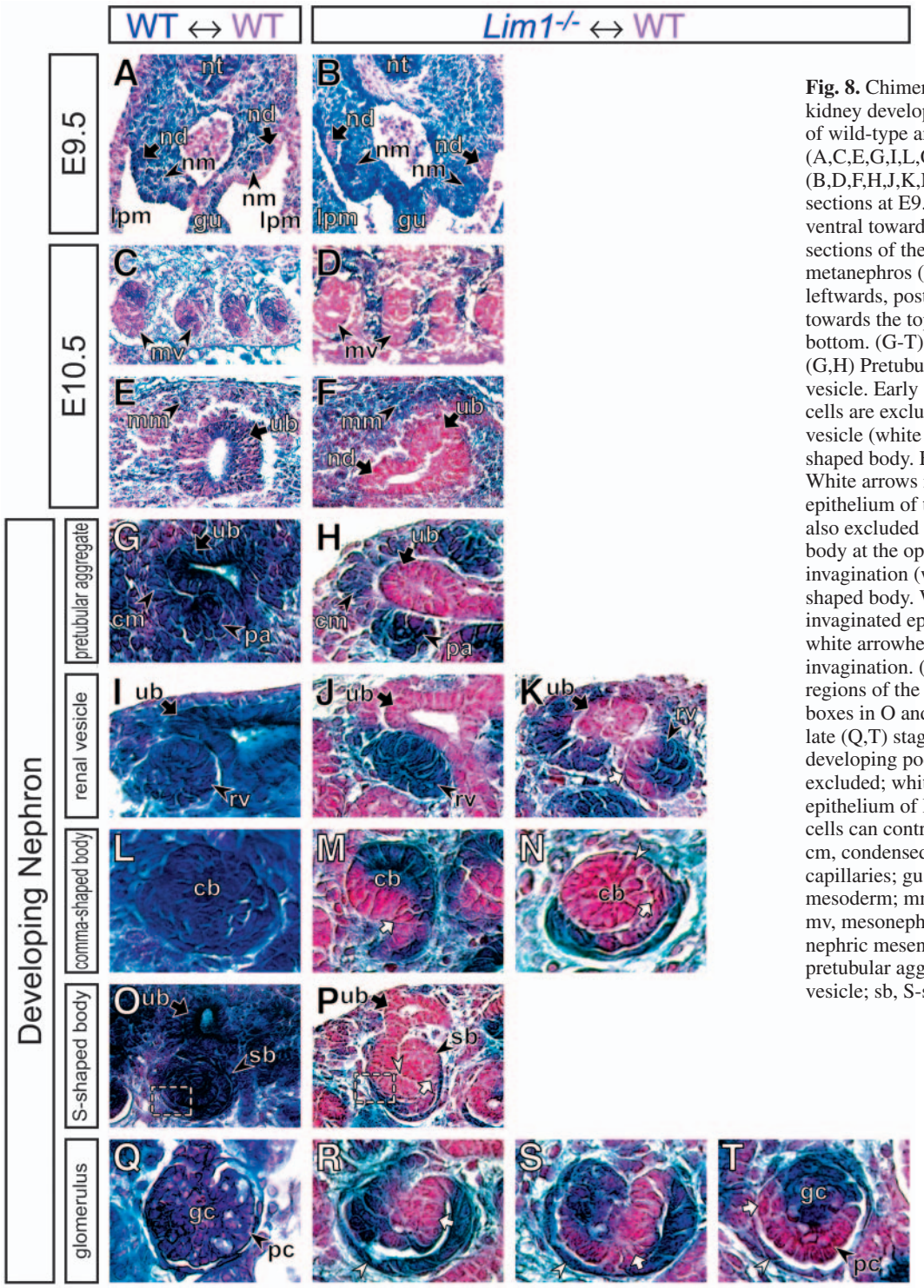

Fig. 8. Chimera analysis of *Lim1* functions in kidney development. Chimeric mice composed of wild-type and *Lim1*$^{+/+}$; *Rosa26*$^{tg/+}$ (A,C,E,G,I,L,O,Q) or *Lim1*$^{-/-}$; *Rosa26*$^{tg/+}$ (B,D,F,H,J,K,M,N,P,R,S,T) cells. (A,B) Cross-sections at E9.5. Dorsal is towards the top and ventral towards the bottom. (C-F) Sagittal sections of the mesonephros (C,D) and metanephros (E,F) regions at E10.5. Anterior is leftwards, posterior rightwards, dorsal is towards the top and ventral is towards the bottom. (G-T) Developing nephrons at E18.5. (G,H) Pretubular aggregate. (I-K) Renal vesicle. Early (J) and late (K) stages. *Lim1*$^{-/-}$ cells are excluded in a subregion of the renal vesicle (white arrow in K). (L-N) Comma-shaped body. Early (M) and late (N) stages. White arrows indicate the invaginating epithelium of the first cleft. *Lim1*$^{-/-}$ cells are also excluded from a part of the comma-shaped body at the opposite side of the epithelial invagination (white arrowhead in N). (O,P) S-shaped body. White arrow indicates invaginated epithelium originally formed; white arrowhead indicates newly formed invagination. (Q-T) Glomerulus (proximal regions of the developing nephron indicated by boxes in O and P). Early (R), middle (S) and late (Q,T) stages. White arrows indicate the developing podocyte where *Lim1*$^{-/-}$ cells are excluded; white arrowheads indicate the outer epithelium of Bowman's capsule where *Lim1*$^{-/-}$ cells can contribute. cb, comma-shaped body; cm, condensed mesenchyme; gc, glomerular capillaries; gu, gut; lpm, lateral plate mesoderm; mm, metanephric mesenchyme; mv, mesonephric vesicle; nd, nephric duct; nm, nephric mesenchyme; nt, neural tube; pa, pretubular aggregate; pc, podocyte; rv, renal vesicle; sb, S-shaped body; ub, ureteric bud.

Wnt4-null mice can form a few glomeruli, nephron tubules and medulla-like structures (Fig. 5D,H), which are completely absent in *Rarb2-Cre*$^{tg/+}$; *Lim1*$^{lz/flox}$ mutant mice.

We found that *Wnt4* expression in the pretubular aggregate (Fig. 7C; data not shown) is broader than *Lim1* expression, which is restricted only in the presumptive renal vesicle (see Fig. S1 in the supplementary material). Although *Lim1-lacZ* expression in nephron progenitors on a *Wnt4*-null background was absent at E12.5 (Fig. 5T), we observed a few *Lim1-lacZ*-positive developing nephrons in *Wnt4*-null mutants later at E14.5 (Fig. 5L,P).

Lim1 function is required for renal vesicle patterning

During nephron development, *Wnt4*, *Pax8* and *Fgf8* expression are initiated in the pretubular aggregate and persist in the renal vesicles (Fig. 7A,C; data not shown) (Stark et al., 1994). In the *Rarb2-Cre*$^{tg/+}$; *Lim1*$^{lz/flox}$ mutants, the expression patterns of *Wnt4*, *Pax8* and *Fgf8* are correctly induced and persist in the

renal vesicle (Fig. 7B,D; data not shown). *Dll1* expression is initially expressed very weakly in the renal vesicle and *Dll1* expression is upregulated in a subset of cells in the renal vesicle during its maturation and persists in the presumptive proximal tubule of the S-shaped body (Fig. 7E,G; data not shown) (Leimeister et al., 2003). In the *Rarb2-Cre*$^{tg/+}$*; Lim1*$^{lz/flox}$ mutants, the upregulation of *Dll1* expression was not observed (Fig. 7F,H). Expression of *Brn1* (also known as *Pou3f3*) is initiated in a subset of cells in the renal vesicle proximal to the ureteric bud and its function is required for the loop of Henle and distal tubule (Fig. 7I; data not shown) (Nakai et al., 2003). In the renal vesicles of the *Rarb2-Cre*$^{tg/+}$*; Lim1*$^{lz/flox}$ mutants, the polarized *Brn1* expression was not observed (Fig. 7J). Expression patterns of a ureteric bud marker *Wnt9b* (Fig. 7K,L) and a stroma marker *Bf2* (Fig. 7M,N) did not change in the *Rarb2-Cre*$^{tg/+}$*; Lim1*$^{lz/flox}$ mutants.

Lim1 acts cell-autonomously in multiple steps during kidney development

To obtain more information about *Lim1* function during kidney development, we performed a chimera analysis (Tam and Rossant, 2003). To generate chimeric mice, we injected *Lim1*$^{-/-}$*; Rosa26*$^{tg/+}$ embryonic stem (ES) cells into wild-type blastocysts (Shawlot et al., 1999). Subsequently, we examined the distribution of *Lim1*-null cells by *lacZ* expression in the chimeric embryos. In control experiments, *Lim1*$^{+/+}$*; Rosa26*$^{tg/+}$ ES cells were injected into wild-type blastocysts. Chimeric kidneys from 57 embryos were analyzed. In control chimeras, *Lim1*$^{+/+}$ cells could extensively contribute to all cell types in the urogenital systems (Fig. 8A,C,E,G,I,L,O,Q).

We found that *Lim1*$^{-/-}$ cells could not contribute to the epithelium of the nephric duct in chimeric mice at E9.5 (Fig. 8B). By contrast, *Lim1*$^{-/-}$ cells could contribute to the nephric mesenchyme at the same stage (Fig. 8B). In the caudal mesonephros of chimeric mice at the E10.5, *Lim1*$^{-/-}$ cells were excluded from the epithelial renal vesicles of the mesonephros (Fig. 8D). The renal vesicles of the caudal mesonephros are derived from the nephric mesenchyme (Fig. 2H), where *Lim1*$^{-/-}$ cells could contribute one day before at E9.5 (Fig. 8B). At the posterior end of the nephric duct at E10.5, *Lim1*$^{-/-}$ cells could contribute to the metanephric mesenchyme, although *Lim1*$^{-/-}$ cells remained excluded from the ureteric bud, which is derived from the nephric duct epithelium (Fig. 8F). These findings suggest that *Lim1* acts cell autonomously for epithelium development of the nephric duct by E9.5 and for renal vesicle formation in the mesonephros between E9.5 and E10.5.

At later stages of development, *Lim1*$^{-/-}$ cells could contribute to the condensed mesenchyme and pretubular aggregate in the metanephros (Fig. 8H). Although *Lim1*$^{-/-}$ cells could initially contribute to the renal vesicle at early stages (Fig. 8J), *Lim1*$^{-/-}$ cells were not found in the region of the renal vesicle proximal to the ureteric bud (Fig. 8K), although *Lim1* is expressed in the entire renal vesicle at this stage (see Fig. S1 in the supplementary material; data not shown) (Karavanov et al., 1998). The epithelial tissue of the renal vesicle that lacks *Lim1*$^{-/-}$ cells invaginates to form the cleft of the comma-shaped body (Fig. 8M,N). Subsequently, *Lim1*$^{-/-}$ cells were not present in the region opposite to the first cleft of differentiating comma-shaped bodies (Fig. 8N, white arrow), which subsequently invaginates to form the second cleft of the S-shaped body (Fig. 8P). *Lim1*$^{-/-}$ cells could contribute to the proximal tip of the S-shaped body (Fig. 8P, dashed box). Subsequently, *Lim1*$^{-/-}$ cells were not found in a subset of cells that faces towards the cleft within the proximal tip of the S-shaped body (Fig. 8R). This small epithelial tissue where *Lim1*$^{-/-}$ cells could not contribute expanded extensively and formed podocytes of the glomerulus (Fig. 8S,T). *Lim1*$^{-/-}$ cells could contribute to the glomerular capillaries and outer epithelium layer of Bowman's capsule (Fig. 8T).

Discussion

The LIM-class homeobox gene *Lim1* is expressed in tubule-forming tissues of the pronephros, mesonephros and metanephros, and genital ducts (Barnes et al., 1994; Fujii et al., 1994; Shawlot and Behringer, 1995). *Lim1*-null neonates lack the urogenital system, including the metanephros, ureter, and male and female reproductive tracts, demonstrating a fundamental role in kidney and genital tract formation (Kobayashi et al., 2004; Shawlot and Behringer, 1995). However, the requirement of *Lim1* for nephric duct formation has hindered an understanding of its later roles in kidney development (Tsang et al., 2000). Here, we demonstrate that *Lim1* is required at multiple steps of kidney development.

Hypomorphic phenotypes in BAC transgene-rescued *Lim1* mutants

It is likely that the 208 kb BAC clone contains most, if not all, tissue-specific transcriptional enhancer elements for *Lim1* expression. It is currently unclear why none of our BAC transgenes could completely rescue the defects of *Lim1*-null mutants. Perhaps overexpression of *Lim1* and/or other genes from the BAC clone during embryogenesis or after birth is lethal, leading to a pre-selection for lower expressing transgenic mice. These BAC transgene rescue findings suggest that *Lim1* function is dose sensitive, i.e. higher expression levels of *Lim1* are required for nephron formation.

Nephric duct epithelium- and metanephric mesenchyme fates during kidney organogenesis

Although the *Hoxb7-Cre* mouse line used in our study was previously generated for Cre-mediated gene manipulations in the nephric duct and ureteric bud (Basson et al., 2005; Rubera et al., 2003; Yu et al., 2002), there was no Cre mouse line specifically for the metanephric mesenchyme, but not in the ureteric bud, from its early stage of development (Bouchard et al., 2004; Ohyama and Groves, 2004; Oxburgh et al., 2004). In this study, we generated a novel resource for metanephric mesenchyme-specific gene modifications, the *Rarb2-Cre* mouse. These two transgenic mouse lines will serve as basic tools to dissect tissue-specific gene functions in the ureteric bud or metanephric mesenchyme.

In the metanephros, *Rarb2* gene expression is restricted to the kidney stroma (Batourina et al., 2001; Mendelsohn et al., 1999). The 4.8 kb *Rarb2* sequences that we used to generate the *Rarb2-Cre* transgenic mouse line were previously tested with a *lacZ* reporter; however, *Rarb2-lacZ* transgenes did not direct metanephric mesenchyme-specific expression (Dolle et al., 1990; Mendelsohn et al., 1991; Reynolds et al., 1991; Shen et al., 1992). Thus, we were surprised to find that our *Rarb2-Cre* transgenic mouse line directed Cre reporter expression in

metanephric mesenchyme and its derivatives. One possibility is that the Cre reporter assay is more sensitive than a *lacZ* transgene. Alternatively, sequences around the site of *Rarb2-Cre* transgene integration were either permissive or fortuitously provided enhancer elements for expression in the metanephric mesenchyme.

Recombinase reporter systems can be used for cell-lineage analysis and fate mapping (Lewandoski, 2001). Recently, it has been suggested that some glomerular capillary cells may derive from the metanephric mesenchyme (Woolf and Loughna, 1998). However, there was no definitive cell-lineage analysis for these cell types. In this study, we found that glomerular capillary cells were Cre reporter negative in *Hoxb7-Cre*; *R26R* and *Rarb2-Cre*; *R26R* mice, suggesting that glomerular capillaries are not derived from either the ureteric bud or metanephric mesenchyme. Similar observations were obtained for the medullary stromal cells. We suggest that glomerular capillary and medullary stromal cells are derived from precursors that arise outside of the ureteric bud and metanephric mesenchyme and that these precursor cells migrate into the developing metanephros after E10.5 in the mouse. Consistent with this idea, it is known that endothelial cells do not form when ureteric bud and metanephric mesenchyme are isolated from embryos at E10.5, recombined, and cultured in vitro to form nephrons (Vainio and Lin, 2002).

Wolffian duct supports Müllerian duct elongation and maintenance

It is widely believed that the upper region of the vagina derives from the Müllerian duct and the lower part from the urogenital sinus (Forsberg, 1973). However, a recent study suggests that the entire vagina derives from the Müllerian duct (Drews et al., 2002). In this study, we found that loss of the posterior part of the Müllerian duct causes the complete loss of the vagina. One explanation is that the entire vagina derives from the Müllerian duct. Alternatively, the urogenital sinus may be induced by the Müllerian duct to form the lower region of the vagina.

During embryogenesis, the Wolffian duct forms first, and subsequently the Müllerian duct forms adjacent to the Wolffian duct (Kobayashi and Behringer, 2003). Experimental interruption of the Wolffian duct in chick embryos resulted in Müllerian duct growth defects (Gruenwald, 1941); however, it is unclear how the Wolffian duct is required for Müllerian duct development. Our data suggest that the Wolffian duct is essential for both elongation and maintenance of the Müllerian duct, but not for initiation.

Distinct tissue-specific *Lim1* functions in kidney development

It has previously been shown that *Lim1* is essential for proper nephric duct formation (Tsang et al., 2000). Here, we found that *Lim1* function is also required for maintenance of the nephric duct after its formation. Furthermore, tubule formation of the caudal mesonephros from the nephric mesenchyme is also disturbed when *Lim1* is inactivated in the nephric duct epithelium. These data suggest that there are nephric duct-derived inductive molecules for mesonephric tubule formation from mesonephric mesenchyme.

Using the *Hoxb7-Cre* and *Rarb2-Cre* transgenic mouse lines, we could dissect *Lim1* functions tissue specifically in the ureteric bud- and metanephric mesenchyme-derived tissues, respectively. Although both tissue-specific mutants have hypoplastic kidneys, *Hoxb7-Cre; Lim1* mutants are alive and have metanephroi with all structures but with abnormal ureter development, whereas *Rarb2-Cre; Lim1* mutants are lethal at birth and have metanephroi without nephrons but with a proper ureteric branching pattern. These observations also indicate that *Lim1* functions within these two tissues may be largely independent during metanephros development. Consistent with this idea, the metanephros of *Hoxb7-Cre*$^{tg/+}$*; Rarb2-Cre*$^{tg/+}$*; Lim1*$^{lz/flox}$ mutants was as small as *Hoxb7-Cre; Lim1* mutants and lacked nephrons in the same way as did *Rarb2-Cre; Lim1* mutants (A.K., unpublished), indicating that defects of *Lim1* mutants in ureteric bud- and metanephric mesenchyme-derived tissues are additive rather than synergistic.

Lim1 in nephric duct-derived tissues for ureteric bud development

Ureteric bud growth and branching is severely perturbed in *Ret* mutants (Schuchardt et al., 1994), whereas *Wnt11* mutants have relatively moderate defects in ureteric bud development (Majumdar et al., 2003). It has also been shown that *Wnt11* and *Gdnf/Ret* pathways synergistically interact with each other in ureteric bud development (Majumdar et al., 2003). In *Hoxb7-Cre; Lim1* mutants, upregulation of *Ret* expression was not observed in the ureteric bud tip, although *Wnt11* expression was normally initiated and maintained. Consistent with these expression patterns, the metanephros was more hypoplastic and ureteric bud growth is severely disturbed in *Hoxb7-Cre; Lim1* mutants compared with those in *Wnt11* mutants. Thus, *Lim1* may act as an upstream regulator for upregulation of *Ret* expression in the ureteric bud tips to regulate ureteric bud growth. Indeed, *Lim1* and *Ret* expression patterns are similar in the developing ureteric bud with highest levels at the ureteric bud tips.

Retinoic acid receptor (Rar) genes in the stromal component are required for *Ret* expression in the ureteric bud (Batourina et al., 2001). It is unlikely that *Lim1* functions through the stroma because *Lim1* is required to upregulate *Ret* at E10.5 before Rar gene expression initiates in the stromal components around E11. Consistent with this idea, *Bf2*-positive stromal components are normally formed in *Hoxb7-Cre; Lim1* mutants at E11.5 (data not shown).

Lim1 function in metanephric mesenchyme-derived tissues for nephron development

The basic unit of the kidney, the nephron, is a long tubule with highly specialized domains, including the glomerulus, distal and proximal tubules, and loop of Henle. It is not clear how the complicated tubular structure of the nephron develops from a simple epithelial sphere, the renal vesicle. Here, we show that *Lim1* is required for the initial step of nephron patterning, renal vesicle patterning. Our chimera analysis indicates that successive cell-autonomous *Lim1* function is also required for comma- to S-shape body morphogenesis and podocyte development.

Although *Lim1* is homogeneously expressed in the renal vesicle, comma-shaped bodies and Bowman's capsule of immature glomeruli, our chimera analysis revealed that *Lim1* function is cell-autonomously required only in specific subregions in these tissues. This may indicate that *Lim1* expression establishes a permissive tissue identity that can

respond to unidentified regional signals that induce epithelial tissues to undergo morphological changes. Indeed, involution of the renal vesicle to form the comma-shaped body is initiated at the same region relative to the position of the ureteric bud, indicating instructive signals that determine renal vesicle patterning emanate from the ureteric tip or stalk, or the surrounding stroma.

Brn1 is essential for development of the distal tubule and loop of Henle (Nakai et al., 2003) and Notch signaling is required for formation of the proximal tubules, podocytes and glomerular capillaries (Cheng et al., 2003; McCright et al., 2001; Wang et al., 2003). Expression of these genes is restricted to a subset of cells in the renal vesicle, but we found that *Brn1* and a component in Notch signaling pathway, *Dll1*, are not expressed in the renal vesicle of *Rarb2-Cre; Lim1* mutants. These observations indicate that regional identities already established at the renal vesicle stage are not present in the absence of *Lim1* function and the loss of these cell types may block further nephrogenesis.

Relationship between *Lim1* and *Wnt4* in nephron development

Lim1 and *Wnt4* are co-expressed in developing nephrons, leading to the idea that these genes may act in the same pathway for pretubular aggregate development (Sariola, 2002). Surprisingly, we found nephrons and developing nephrons in the hypoplastic kidneys of neonatal and E14.5 *Wnt4*-null mutants, respectively. However, at E12.5 no developing nephrons were found in *Wnt4*-null mutants. Our observations are somewhat contrary to a previous report, indicating that *Wnt4* is essential for the mesenchyme-to-epithelial transition during nephron development (Stark et al., 1994). This may be because of genetic background differences between the mice used in the two studies, indicating genetic modifiers that regulate nephron development in the absence of *Wnt4*.

The *Wnt4* expression pattern in the pretubular aggregate is broader than the *Lim1* expression pattern, which is restricted to the presumptive renal vesicle, and *Lim1* expression is not detected in the pretubular aggregate of *Wnt4*-null mutants at early stages. This indicates that *Wnt4* may function at an early stage of pretubular aggregate differentiation before *Lim1* expression initiates in this tissue. It is possible that *Lim1* and *Wnt4* may regulate independent pathways in nephron progenitors. Alternatively, *Wnt4* is essential for the normal onset of nephrogenesis acting as an upstream factor for *Lim1* expression, but a *Wnt4*-independent process that upregulates *Lim1* can give rise to a limited number of nephrons in *Wnt4*-null kidneys.

In addition to reduced and delayed nephron development, the growth of the metanephros and development of the ureteric bud is severely retarded in *Wnt4* mutants compared with *Rarb2-Cre*$^{tg/+}$*; Lim1*$^{lz/flox}$ mutants, in which metanephros growth and ureteric bud branching are relatively normal even when nephrons are completely absent. These data suggest that renal vesicles, which *Wnt4*-null mutants essentially lack, may transmit promoting signals to regulate kidney growth and ureteric bud development. Alternatively, *Wnt4* in the pretubular aggregate itself may also be the promoting signal for ureteric bud development.

Lim1 is a primary genetic factor for amniote kidney organogenesis

The embryonic development of the three successive kidneys of amniotes recapitulates the evolution of this organ system (Saxen, 1987). Whereas there are many genes with restricted expression patterns in diverse tissues and stages that regulate one particular aspect of kidney development, there are very few genes that are expressed in each of the three kidney types (Vainio and Lin, 2002). A small set of transcription factors (Pax2, Pax8 and Lim1) are expressed in tubule-forming tissues in each of the three kidney types. Mutants for *Lim1* and *Pax2* have nephric duct defects that lead to an absence of mesonephros and metanephros development (Bouchard et al., 2004; Shawlot et al., 1999; Torres et al., 1995; Tsang et al., 2000). *Pax8* mutants do not have kidney defects but genetic studies indicate that *Pax2* and *Pax8* act redundantly for nephric duct formation, perhaps upstream of *Lim1* (Bouchard et al., 2002; Mansouri et al., 1998). In addition, overexpression of both *XPax-8* and *XLim-1* together in frog embryos leads to embryonic kidney overgrowth and ectopic pronephric tubules (Carroll and Vize, 1999). The results presented here and by others suggest that *Lim1* is crucially required in the tubule-forming tissues at multiple steps of kidney development. Although the precise relationships between *Pax2*, *Pax8* and *Lim1* are complex, it is clear that they are each used at multiple steps of kidney organogenesis.

The development of the amniote excretory system (pronephros, mesonephros, and metanephros) suggests that it has evolved by elaborating on a fundamental developmental process, tubulogenesis. A simple way to evolve such an organ system would be to use that process repeatedly and exploit a fundamental genetic program. It would appear that the set of transcription factors mentioned above serves as a fundamental genetic cassette for tubulogenesis during kidney development. Interestingly, the mechanism regulated by *Lim1* for nephric duct, Wolffian and Müllerian duct, mesonephric tubule and ureteric bud formation appear to be similar, i.e. a cell-autonomous action for maintenance and/or growth of the ductal epithelium. However, this mechanism appears to be fundamentally different for nephron formation, i.e. formation of a permissive tissue identity, resulting in regional patterning of the renal vesicle for subsequent morphogenesis. Thus, it would appear that a new elaboration of our proposed primary genetic cassette evolved for nephron formation in the metanephros. This may have been facilitated by the ability of LIM-class homeodomain proteins to complex with other factors to regulate transcription (Bach et al., 1997).

We thank William Shawlot for *Lim1*$^{+/+}$*; R26*$^{tg/+}$ and *Lim1*$^{-/-}$*; R26*$^{tg/+}$ ES cells, Artur Kania and Thomas Jessell for *Lim1*$^{lz/+}$ mice, Allan Bradley for SNL 76/7 STO cells, and Robert McEvilly, Frank Costantini, Achim Gossler, Brigid Hogan and Peter Gruss for probes. These studies were supported by a grant from the National Institutes of Health (NIH) HD30284 to R.R.B., by DK61459 and DK55388 to C.M., and by DK054363 to A.P.M. DNA sequencing and veterinary resources were supported by the NIH Cancer Center Support Grant CA16672.

Supplementary material

Supplementary material for this article is available at
http://dev.biologists.org/cgi/content/full/132/12/2809/DC1

References

Bach, I., Carriere, C., Ostendorff, H. P., Andersen, B. and Rosenfeld, M. G. (1997). A family of LIM domain-associated cofactors confer transcriptional synergism between LIM and Otx homeodomain proteins. *Genes Dev.* **11**, 1370-1380.

Bard, J. B., Gordon, A., Sharp, L. and Sellers, W. I. (2001). Early nephron formation in the developing mouse kidney. *J. Anat.* **199**, 385-392.

Barnes, J. D., Crosby, J. L., Jones, C. M., Wright, C. V. and Hogan, B. L. (1994). Embryonic expression of Lim-1, the mouse homolog of *Xenopus* Xlim-1, suggests a role in lateral mesoderm differentiation and neurogenesis. *Dev. Biol.* **161**, 168-178.

Basson, M. A., Akbulut, S., Watson-Johnson, J., Simon, R., Carroll, T. J., Shakya, R., Gross, I., Martin, G. R., Lufkin, T. and McMahon, A. P. (2005). Sprouty1 is a critical regulator of GDNF/RET-mediated kidney induction. *Dev. Cell* **8**, 229-239.

Batourina, E., Gim, S., Bello, N., Shy, M., Clagett-Dame, M., Srinivas, S., Costantini, F. and Mendelsohn, C. (2001). Vitamin A controls epithelial/mesenchymal interactions through Ret expression. *Nat. Genet.* **27**, 74-78.

Batourina, E., Choi, C., Paragas, N., Bello, N., Hensle, T., Costantini, F. D., Schuchardt, A., Bacallao, R. L. and Mendelsohn, C. L. (2002). Distal ureter morphogenesis depends on epithelial cell remodeling mediated by vitamin A and Ret. *Nat. Genet*. **32**, 109-115.

Bouchard, M., Souabni, A., Mandler, M., Neubuser, A. and Busslinger, M. (2002). Nephric lineage specification by Pax2 and Pax8. *Genes Dev.* **16**, 2958-2970.

Bouchard, M., Souabni, A. and Busslinger, M. (2004). Tissue-specific expression of cre recombinase from the Pax8 locus. *Genesis* **38**, 105-109.

Carroll, T. J. and Vize, P. D. (1999). Synergism between Pax-8 and lim-1 in embryonic kidney development. *Dev. Biol.* **214**, 46-59.

Carroll, T. J. and McMahon, A. P. (2003). Overview: the molecular basis of kidney development. In *The kidney* (ed. P. D. Vize, A. S. Woolf and J. B. L. Bard), pp. 343-376. London: Academic Press.

Cheng, H. T., Miner, J. H., Lin, M., Tansey, M. G., Roth, K. and Kopan, R. (2003). Gamma-secretase activity is dispensable for mesenchyme-to-epithelium transition but required for podocyte and proximal tubule formation in developing mouse kidney. *Development* **130**, 5031-5042.

Davies, J. (2001). Intracellular and extracellular regulation of ureteric bud morphogenesis. *J. Anat.* **198**, 257-264.

Davies, J. A. and Davey, M. G. (1999). Collecting duct morphogenesis. *Pediatr. Nephrol.* **13**, 535-541.

Dolle, P., Ruberte, E., Leroy, P., Morriss-Kay, G. and Chambon, P. (1990). Retinoic acid receptors and cellular retinoid binding proteins. I. A systematic study of their differential pattern of transcription during mouse organogenesis. *Development* **110**, 1133-1151.

Dressler, G. (2002). Tubulogenesis in the developing mammalian kidney. *Trends Cell Biol.* **12**, 390-395.

Drews, U., Sulak, O. and Schenck, P. A. (2002). Androgens and the development of the vagina. *Biol. Reprod.* **67**, 1353-1359.

Forsberg, J. G. (1973). Cervicovaginal epithelium: its origin and development. *Am. J. Obstet. Gynecol.* **115**, 1025-1043.

Fujii, T., Pichel, J. G., Taira, M., Toyama, R., Dawid, I. B. and Westphal, H. (1994). Expression patterns of the murine LIM class homeobox gene *lim1* in the developing brain and excretory system. *Dev. Dyn.* **199**, 73-83.

Grobstein, C. (1953). Inductive epitheliomesenchymal interaction in cultured organ rudiments of the mouse. *Science* **118**, 52-55.

Grobstein, C. (1956). Trans-filter induction of tubules in mouse metanephrogenic mesenchyme. *Exp. Cell Res.* **10**, 424-440.

Gruenwald, P. (1941). The relation of the growing Mullerian duct to the Wolffian duct and its importance for the genesis of malformations. *Anat. Rec.* **81**, 1-19.

Hatini, V., Huh, S. O., Herzlinger, D., Soares, V. C. and Lai, E. (1996). Essential role of stromal mesenchyme in kidney morphogenesis revealed by targeted disruption of Winged Helix transcription factor BF-2. *Genes Dev.* **10**, 1467-1478.

Hogan, B. L. and Kolodziej, P. A. (2002). Organogenesis: molecular mechanisms of tubulogenesis. *Nat. Rev. Genet.* **3**, 513-523.

Kania, A., Johnson, R. L. and Jessell, T. M. (2000). Coordinate roles for LIM homeobox genes in directing the dorsoventral trajectory of motor axons in the vertebrate limb. *Cell* **102**, 161-173.

Karavanov, A. A., Karavanova, I., Perantoni, A. and Dawid, I. B. (1998). Expression pattern of the rat Lim-1 homeobox gene suggests a dual role during kidney development. *Int. J. Dev. Biol.* **42**, 61-66.

Kispert, A., Vainio, S., Shen, L., Rowitch, D. H. and McMahon, A. P. (1996). Proteoglycans are required for maintenance of Wnt-11 expression in the ureter tips. *Development* **122**, 3627-3637.

Kobayashi, A. and Behringer, R. R. (2003). Developmental genetics of the female reproductive tract in mammals. *Nat. Rev. Genet.* **4**, 969-980.

Kobayashi, A., Shawlot, W., Kania, A. and Behringer, R. R. (2004). Requirement of Lim1 for female reproductive tract development. *Development* **131**, 539-549.

Kume, T., Deng, K. and Hogan, B. L. (2000). Murine forkhead/winged helix genes Foxc1 (Mf1) and Foxc2 (Mfh1) are required for the early organogenesis of the kidney and urinary tract. *Development* **127**, 1387-1395.

Kuure, S., Vuolteenaho, R. and Vainio, S. (2000). Kidney morphogenesis: cellular and molecular regulation. *Mech. Dev.* **92**, 31-45.

Kwan, K. M. (2002). Conditional alleles in mice: practical considerations for tissue-specific knockouts. *Genesis* **32**, 49-62.

Kwan, K. M. and Behringer, R. R. (2002). Conditional inactivation of Lim1 function. *Genesis* **32**, 118-120.

Lechner, M. S. and Dressler, G. R. (1997). The molecular basis of embryonic kidney development. *Mech. Dev.* **62**, 105-120.

Leimeister, C., Schumacher, N. and Gessler, M. (2003). Expression of Notch pathway genes in the embryonic mouse metanephros suggests a role in proximal tubule development. *Gene Expr. Patterns* **3**, 595-598.

Lewandoski, M. (2001). Conditional control of gene expression in the mouse. *Nat. Rev. Genet* **2**, 743-755.

Lubarsky, B. and Krasnow, M. A. (2003). Tube morphogenesis: making and shaping biological tubes. *Cell* **112**, 19-28.

Majumdar, A., Vainio, S., Kispert, A., McMahon, J. and McMahon, A. P. (2003). Wnt11 and Ret/Gdnf pathways cooperate in regulating ureteric branching during metanephric kidney development. *Development* **130**, 3175-3185.

Mansouri, A., Chowdhury, K. and Gruss, P. (1998). Follicular cells of the thyroid gland require Pax8 gene function. *Nat. Genet.* **19**, 87-90.

McCright, B., Gao, X., Shen, L., Lozier, J., Lan, Y., Maguire, M., Herzlinger, D., Weinmaster, G., Jiang, R. and Gridley, T. (2001). Defects in development of the kidney, heart and eye vasculature in mice homozygous for a hypomorphic Notch2 mutation. *Development* **128**, 491-502.

Mendelsohn, C., Ruberte, E., LeMeur, M., Morriss-Kay, G. and Chambon, P. (1991). Developmental analysis of the retinoic acid-inducible RAR-beta 2 promoter in transgenic animals. *Development* **113**, 723-734.

Mendelsohn, C., Batourina, E., Fung, S., Gilbert, T. and Dodd, J. (1999). Stromal cells mediate retinoid-dependent functions essential for renal development. *Development* **126**, 1139-1148.

Miyamoto, N., Yoshida, M., Kuratani, S., Matsuo, I. and Aizawa, S. (1997). Defects of urogenital development in mice lacking Emx2. *Development* **124**, 1653-1664.

Moore, M. W., Klein, R. D., Farinas, I., Sauer, H., Armanini, M., Phillips, H., Reichardt, L. F., Ryan, A. M., Carver-Moore, K. and Rosenthal, A. (1996). Renal and neuronal abnormalities in mice lacking GDNF. *Nature* **382**, 76-79.

Nagy, A. (2000). Cre recombinase: the universal reagent for genome tailoring. *Genesis* **26**, 99-109.

Nagy, A., Gertsenstein, M., Vintersten, K. and Behringer, R. R. (2003). *Manipulating the Mouse Embryo: A Laboratory Manual.* Cold Spring Harbor: Cold Spring Harbor Laboratory Press.

Nakai, S., Sugitani, Y., Sato, H., Ito, S., Miura, Y., Ogawa, M., Nishi, M., Jishage, K., Minowa, O. and Noda, T. (2003). Crucial roles of Brn1 in distal tubule formation and function in mouse kidney. *Development* **130**, 4751-4759.

Obara-Ishihara, T., Kuhlman, J., Niswander, L. and Herzlinger, D. (1999). The surface ectoderm is essential for nephric duct formation in intermediate mesoderm. *Development* **126**, 1103-1108.

Ohyama, T. and Groves, A. K. (2004). Generation of Pax2-Cre mice by modification of a Pax2 bacterial artificial chromosome. *Genesis* **38**, 195-199.

Oxburgh, L., Chu, G. C., Michael, S. K. and Robertson, E. J. (2004). TGFbeta superfamily signals are required for morphogenesis of the kidney mesenchyme progenitor population. *Development* **131**, 4593-4605.

Pichel, J. G., Shen, L., Sheng, H. Z., Granholm, A. C., Drago, J., Grinberg, A., Lee, E. J., Huang, S. P., Saarma, M., Hoffer, B. J. et al. (1996). Defects in enteric innervation and kidney development in mice lacking GDNF. *Nature* **382**, 73-76.

Pohl, M., Stuart, R. O., Sakurai, H. and Nigam, S. K. (2000). Branching morphogenesis during kidney development. *Annu. Rev. Physiol.* **62**, 595-620.

Reynolds, K., Mezey, E. and Zimmer, A. (1991). Activity of the beta-retinoic acid receptor promoter in transgenic mice. *Mech. Dev.* **36**, 15-29.

Rubera, I., Loffing, J., Palmer, L. G., Frindt, G., Fowler-Jaeger, N., Sauter,

D., Carroll, T., McMahon, A., Hummler, E. and Rossier, B. C. (2003). Collecting duct-specific gene inactivation of alphaENaC in the mouse kidney does not impair sodium and potassium balance. *J. Clin. Invest.* **112**, 554-565.
Sainio, K. and Raatikainen-Ahokas, A. (1999). Mesonephric kidney – a stem cell factory? *Int. J. Dev. Biol.* **43**, 435-439.
Sainio, K., Hellstedt, P., Kreidberg, J. A., Saxen, L. and Sariola, H. (1997). Differential regulation of two sets of mesonephric tubules by WT-1. *Development* **124**, 1293-1299.
Sanchez, M. P., Silos-Santiago, I., Frisen, J., He, B., Lira, S. A. and Barbacid, M. (1996). Renal agenesis and the absence of enteric neurons in mice lacking GDNF. *Nature* **382**, 70-73.
Sariola, H. (2002). Nephron induction revisited: from caps to condensates. *Curr. Opin. Nephrol. Hypertens.* **11**, 17-21.
Sauer, B. and Henderson, N. (1990). Targeted insertion of exogenous DNA into the eukaryotic genome by the Cre recombinase. *New Biol.* **2**, 441-449.
Saxen, L. (1987). *Organogenesis of the Kidney*. New York: Cambridge University Press.
Schuchardt, A., D'Agati, V., Larsson-Blomberg, L., Costantini, F. and Pachnis, V. (1994). Defects in the kidney and enteric nervous system of mice lacking the tyrosine kinase receptor Ret. *Nature* **367**, 380-383.
Shah, M. M., Sampogna, R. V., Sakurai, H., Bush, K. T. and Nigam, S. K. (2004). Branching morphogenesis and kidney disease. *Development* **131**, 1449-1462.
Shawlot, W. and Behringer, R. R. (1995). Requirement for Lim1 in head-organizer function. *Nature* **374**, 425-430.
Shawlot, W., Wakamiya, M., Kwan, K. M., Kania, A., Jessell, T. M. and Behringer, R. R. (1999). Lim1 is required in both primitive streak-derived tissues and visceral endoderm for head formation in the mouse. *Development* **126**, 4925-4932.
Shen, S., van den Brink, C. E., Kruijer, W. and van der Saag, P. T. (1992). Embryonic stem cells stably transfected with mRAR beta 2-lacZ exhibit specific expression in chimeric embryos. *Int. J. Dev. Biol.* **36**, 465-476.
Soriano, P. (1999). Generalized lacZ expression with the ROSA26 Cre reporter strain. *Nat. Genet.* **21**, 70-71.
Stark, K., Vainio, S., Vassileva, G. and McMahon, A. P. (1994). Epithelial transformation of metanephric mesenchyme in the developing kidney regulated by Wnt-4. *Nature* **372**, 679-683.
Tam, P. P. and Rossant, J. (2003). Mouse embryonic chimeras: tools for studying mammalian development. *Development* **130**, 6155-6163.
Torres, M., Gomez-Pardo, E., Dressler, G. R. and Gruss, P. (1995). Pax-2 controls multiple steps of urogenital development. *Development* **121**, 4057-4065.
Tsang, T. E., Shawlot, W., Kinder, S. J., Kobayashi, A., Kwan, K. M., Schughart, K., Kania, A., Jessell, T. M., Behringer, R. R. and Tam, P. P. (2000). Lim1 activity is required for intermediate mesoderm differentiation in the mouse embryo. *Dev. Biol.* **223**, 77-90.
Vainio, S. and Lin, Y. (2002). Coordinating early kidney development: lessons from gene targeting. *Nat. Rev. Genet.* **3**, 533-543.
Wang, P., Pereira, F. A., Beasley, D. and Zheng, H. (2003). Presenilins are required for the formation of comma- and S-shaped bodies during nephrogenesis. *Development* **130**, 5019-5029.
Woolf, A. S. and Loughna, S. (1998). Origin of glomerular capillaries: is the verdict in? *Exp. Nephrol.* **6**, 17-21.
Yu, J., Carroll, T. J. and McMahon, A. P. (2002). Sonic hedgehog regulates proliferation and differentiation of mesenchymal cells in the mouse metanephric kidney. *Development* **129**, 5301-5312.